

**Course Reader
for
Introduction to Solid State Physics**

Di-Jing Huang

© *Draft date September 15, 2014*

Contents

1 Specific Heat of Solids	3
1.1 Einstein's calculation: simple harmonic oscillator	3
1.2 The T^3 dependence	5
2 Electrons in Metals	11
2.1 The Drude model	11
2.2 Free electron Fermi gas	15
2.3 Electronic Heat Capacity	20
2.4 Thermionic Emission of Electrons from Metals	22
3 Vibrations of One-Dimensional Lattices	23
3.1 One-dimensional monatomic solids	23
3.2 Reciprocal lattice	25
3.3 Diaomic chain	28
3.4 Quantized waves: phonons	30
3.5 Thermal expansion	32
3.6 Heat conduction by phonons	32
4 Crystal structure	33
4.1 Lattices and unit cells	33
4.2 Symmetry of 3D crystals	35
4.3 The reciprocal lattice in 3D	39
5 Wave Scattering by Crystals	45
5.1 The Laue and Bragg Conditions	45
6 Electrons in a Periodic Potential	51
6.1 Tight-Binding Approximation	51
6.2 The Translational Symmetry – Bloch's theorem	54
6.3 Nearly Free Electrons	59
6.4 Symmetry in Electronic Band Structure	65

7	Electron-Electron Interactions	67
7.1	The Hatree-Fock approximation	67
7.2	Electron-electron interaction: Screening	67
7.3	Fermi liquid and quasiparticles	67
7.4	Electron-phonon interaction	67
7.5	Electrons in a magnetic Field	67
8	Semiconductor Physics	69
8.1	Electrons and Holes	69
9	Magnetism	71

Introduction

Solid-state physics is the field of physics that deals with the macroscopic and microscopic physical properties of solids, state of matter in which a large number of atoms are chemically bound to produce a dense aggregate. These properties are broad, rich, and deep because they emerge from collective phenomena of enormously large number of particles. This many-body physics is often beyond reductionism and most of the time is closely connected to our daily life.

This course reader is prepared to cover what will be presented in the lecture of *Introduction to Solid State Physics (I)*. Instead of surveying many phenomena of solids, this course focusses on basic concept of solid-state physics, including crystalline lattice structure, electronic properties, semiconductor physics, and magnetism. The contents of this course follow Simon's text closely; symbols and notations used here are almost the same as those in the textbook.

Textbook: The Oxford Solid State Basics, by S. Simon, Oxford University Press (2013)

References:

- Introduction to Solid State Physics, 8th ed, by Charles Kittel, Wiley (2004).

This is a very popular text. It collects many useful informations and is quite handy as a reference material after you have some background in solid state physics. In my opinion, it is not a good introductory book. Its theme may seem unclear to many beginners, particularly those who find themselves struggling to follow its presentation.

- Solid-State Physics, 4th ed, by H. Ibach and H. Luth, Springer-Verlag (2009).

Another very popular book on the subject, with quite a bit of information in it.

Two graduate-level references:

- Solid State Physics by N. W. Ashcroft and D. N. Mermin, Cengage Learning (1976).

This is an elegantly written and standard complete introduction to solid state physics although it is a dated book, published 38 years ago. Still it is a favorite text of many solid-state-physics courses.

- Condensed Matter Physics, 2nd ed, by M. Marder, Wiley (2010).

It is a good reference book which is complementary to the classic Ashcroft-Mermin text; some parts of the book practically echo Ashcroft-Mermin. The author attempts to provide a great deal of breadth on the modern condensed matter physics. The derivations are complete, although difficult for some beginners to follow.

Chapter 1

Specific Heat of Solids

Historically the research of solid state physics began with the study of the thermal properties of solids without considering microscopic structure. In 1819 Dulong and Petit found experimentally that for many solids at room temperature the heat capacity per atom C_v is approximately $3Nk_B$, i.e., the Law of Dulong-Petit, where k_B is Boltzmann's constant. While this law is not always correct, it frequently is correct for most of materials. An exceptional example is diamond whose molar heat capacity at room temperature is $0.735R$, much smaller than $3R$. Particularly this law does not hold at low temperatures; for diamond, room temperature appears be "low" temperature.

1.1 Einstein's calculation: simple harmonic oscillator

Consider an 1D harmonic oscillator in equilibrium with a heat bath at temperature T . The oscillator can not be fixed at a quantum state n with energy $\mathcal{E}_n = \hbar\omega(n + 1/2)$, where \hbar and ω are the Planck constant divided by 2π and the angular frequency, respectively. Instead the probability that the oscillator is in state n is $P_n = \alpha e^{-\beta\mathcal{E}_n}$ in which α is a normalization constant and β is defined as $1/k_B T$ with k_B being the Boltzmann constant. As the oscillator must be in one of the possible states,

$$\begin{aligned} \sum_n P_n &= 1, \\ \alpha \sum_{n=0}^{\infty} e^{-\beta\hbar\omega(n+1/2)} &= \alpha \frac{e^{-\beta\hbar\omega/2}}{1 - e^{-\beta\hbar\omega}} = 1, \\ \alpha &= (1 - e^{-\beta\hbar\omega})e^{\beta\hbar\omega/2}. \end{aligned}$$

Therefore we have

$$P_n = (1 - e^{-\beta \hbar \omega}) e^{-n\beta \hbar \omega} \quad (1.1)$$

and the average energy $\langle \mathcal{E} \rangle$ of the system is

$$\begin{aligned} \langle \mathcal{E} \rangle &= \sum_{n=0}^{\infty} \hbar \omega (n + 1/2) (1 - e^{-\beta \hbar \omega}) e^{-n\beta \hbar \omega} \\ &= \frac{\hbar \omega}{2} + \hbar \omega (1 - e^{-\beta \hbar \omega}) \sum_{n=0}^{\infty} n (e^{-\beta \hbar \omega})^n \\ &= \frac{\hbar \omega}{2} + \hbar \omega (1 - e^{-\beta \hbar \omega}) \frac{e^{-\beta \hbar \omega}}{(1 - e^{-\beta \hbar \omega})^2} \\ &= \hbar \omega \left(\frac{1}{e^{\beta \hbar \omega} - 1} + \frac{1}{2} \right). \end{aligned} \quad (1.2)$$

Here we use $\sum_{n=0}^{\infty} nx^n = \frac{x}{(1-x)^2}$ to calculate the summation.¹ This expression has the form of $E_n = \hbar \omega (n_B + 1/2)$ of a single harmonic oscillator with the Bose occupation factor n_B as

$$n_B(\beta \hbar \omega) = \frac{1}{e^{\beta \hbar \omega} - 1}.$$

and the expectation energy of the "solid" is then²

$$\langle \mathcal{E} \rangle = \hbar \omega \left(n_B(\beta \hbar \omega) + 1/2 \right).$$

The heat capacity C is defined as

$$C = \frac{\partial \langle \mathcal{E} \rangle}{\partial T}.$$

Differentiating $\langle \mathcal{E} \rangle$ with respect to temperature T and defining $x \equiv \beta \hbar \omega$, we then obtain the heat capacity

$$C = \hbar \omega \frac{\partial x}{\partial T} \frac{\partial}{\partial x} \frac{1}{e^x - 1} = k_B (\beta \hbar \omega)^2 \frac{e^{\beta \hbar \omega}}{(e^{\beta \hbar \omega} - 1)^2}. \quad (1.3)$$

In the high-temperature limit, $(e^{\beta \hbar \omega} - 1)$ approaches $\beta \hbar \omega$ because $e^x \approx 1 + x$, we then have $C = k_B$, consistent with the Law of Dulong-Petit.

For the 3D case,

$$\mathcal{E}_{n_x, n_y, n_z} = \hbar \omega \left(n_x + \frac{1}{2} + n_y + \frac{1}{2} + n_z + \frac{1}{2} \right), \quad (1.4)$$

¹It is straightforward to show $\sum_{n=0}^{\infty} nx^n = \frac{x}{(1-x)^2}$ by differentiating the geometric series $\sum_{n=0}^{\infty} x^n = \frac{1}{1-x}$.

²Alternatively see Simon's text for using the 1D partition function $Z_{1D} = \sum_{n \geq 0} e^{-\beta \hbar \omega (n+1/2)}$ and to obtain $\langle \varepsilon \rangle$, because the average energy is $\langle \varepsilon \rangle = -\frac{\partial \ln Z_{1D}}{\partial \beta}$.

and

$$\langle \mathcal{E}_{3D} \rangle = 3\langle \mathcal{E}_{1D} \rangle. \quad (1.5)$$

Consequently the heat capacity is

$$C = 3k_B(\beta\hbar\omega)^2 \frac{e^{\beta\hbar\omega}}{(e^{\beta\hbar\omega} - 1)^2}. \quad (1.6)$$

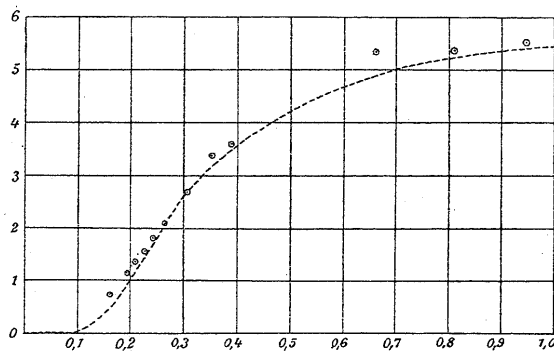


Figure 2.2: Plot of Specific Heat of Diamond from Einstein's original 1907 paper. The fit is to the Einstein theory of heat capacity. The x-axis is $k_B T$ in units of $\hbar\omega$ and y axis is C in units of cal/(K-mol). In these units, $3R \approx 5.96$.

Figure 1.1: C vs T, from Simon's text

As plotted in Fig. 1.1, Einstein's calculation reasonably accurately explained the behavior of the the heat capacity of diamond as a function of temperature with only a single fitting parameter ω , the Einstein frequency. His result was remarkable as it told us that quantum mechanics is important to correctly explain the temperature dependence.

1.2 The T^3 dependence

Einstein successfully explained the molar heat capacity of diamond, but still there were clear deviations from the prediction at low temperatures. For example, Fig. 1.2 shows that the low-temperature heat capacity of solid argon below 2 K is proportional to T^3 .

In 1912 Peter Debye discovered how to better treat the quantum mechanics of oscillations of atoms, and managed to explain the T^3 specific heat. In Debye's model, we have the following assumptions:

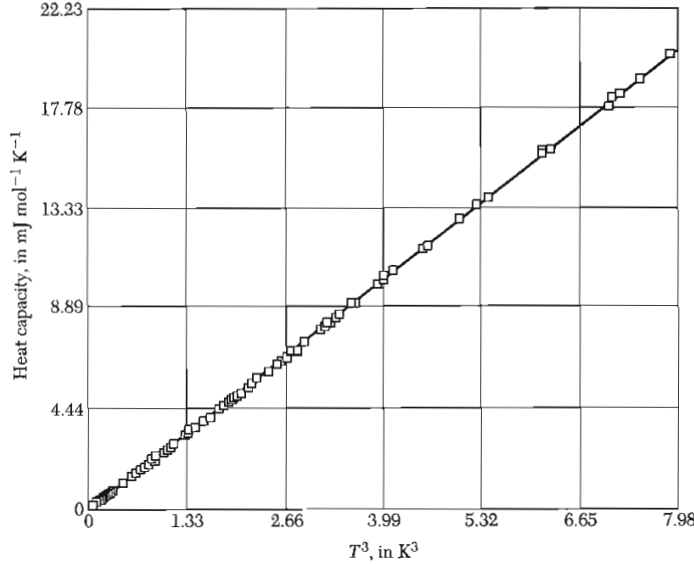


Figure 1.2: Low-temperature heat capacity of solid argon plotted against T^3 , from Kittel's text

- The thermal energy results from sound wave, i.e., vibration of atoms with long wavelength.
- Sound waves in solids are quantized the same way as Planck quantized light waves.
- A linear dispersion of frequency ω versus wave vector k is assumed, i.e., $\omega(\mathbf{k}) = v|\mathbf{k}|$; here v is the sound velocity.
- Vibration of atoms is isotropic; the transverse and longitudinal modes have the same velocity, $v_l = v_t$.
- There is a maximum frequency to obtain a total of $3N$ degrees of freedom of the system.

Now we have the expectation of thermal energy

$$\langle \mathcal{E} \rangle = 3 \sum_{\mathbf{k}} \hbar \omega(\mathbf{k}) \left(n_B(\mathbf{k}) + \frac{1}{2} \right). \quad (1.7)$$

To sum over all possible values of k , we need to replace the summation $\sum_{\mathbf{k}}$ with an integral $\int d\mathbf{k}$.

periodic boundary condition

Consider waves in an 1-D system of length L , e.g., 1D chain of atom with an interatomic spacing a . If the end effects are ignored, the precise way of treating the atoms at the ends is unimportant and we may choose the approach on grounds of mathematical convenience. The most convenient choice is the Born-von Barman periodic boundary condition. Any wave in the sample e^{ikx} is required to have same value for a position x as it for $x + L$, i.e., $e^{ikx} = e^{ik(x+L)}$. This requires $e^{ikL} = 1$ and then restricts k to be certain discrete values

$$k = \frac{2\pi n}{L}$$

for n an integer. The spacing between allowed k point in k space is $\frac{2\pi}{L}$. If $L \gg a$, k is nearly continuous and we can replace a sum over k by an integral. Because $\Delta k = \frac{2\pi}{L}$, we have the following replacement

$$\sum_k \rightarrow \frac{L}{2\pi} \int dk.$$

In three dimensions, we can extend this discretization of values of \mathbf{k} for a sample of size L^3 and obtain

$$\sum_{\mathbf{k}} \rightarrow \frac{L^3}{(2\pi)^3} \int d\mathbf{k}. \quad (1.8)$$

Debye's calculation

Following Eqs. 1.7 and 1.8, we obtain the expectation of thermal energy

$$\langle \mathcal{E} \rangle = 3 \frac{L^3}{(2\pi)^3} \int d\mathbf{k} \hbar \omega(\mathbf{k}) \left(n_B(\mathbf{k}) + \frac{1}{2} \right). \quad (1.9)$$

For $k = \omega/v$ and using the spherical symmetry,³

$$\langle \mathcal{E} \rangle = 3 \frac{4\pi L^3}{(2\pi)^3 v^3} \int_0^\infty \omega^2 d\omega (\hbar\omega) \left(n_B(\beta\hbar\omega) + \frac{1}{2} \right). \quad (1.10)$$

Now we introduce the *density of states* $g(\omega)$ of vibration such that $g(\omega)d\omega$ gives the total number of vibration modes with frequency between ω and $\omega + d\omega$. Then the expectation of thermal energy can be expressed as

$$\langle \mathcal{E} \rangle = \int_0^\infty d\omega (\hbar\omega) g(\omega) \left(n_B(\beta\hbar\omega) + \frac{1}{2} \right), \quad (1.11)$$

³Note that $\int d\mathbf{k} \rightarrow 4\pi \int_0^\infty k^2 dk$.

and the density of states is

$$g(\omega) = \frac{12\pi L^3 \omega^2}{(2\pi)^3 v^3} = N \frac{12\pi}{(2\pi)^3 n} \frac{\omega^2}{v^3} = N \frac{9\omega^2}{\omega_d^3} \quad (1.12)$$

with N the total number of atoms and n the density of atoms. $\omega_d \equiv (6\pi^2 n)^{1/3} v$ is known as the Debye frequency. Therefore the heat capacity is

$$\begin{aligned} C &= \frac{9N\hbar\omega^2}{\omega_d^3} \frac{\partial}{\partial T} \int_0^\infty \frac{\omega^3}{e^{\hbar\omega/k_B T} - 1} d\omega \\ &= \frac{9N\hbar\omega^2 k_B^4}{\omega_d^3 \hbar^4} \frac{\partial}{\partial T} T^4 \int_0^\infty \frac{x^3}{e^x - 1} dx \\ &= Nk_B \frac{12\pi^4}{5} \frac{(k_B T)^3}{(\hbar\omega_d)^3}. \end{aligned} \quad (1.13)$$

Note that one can use the Riemann zeta function $\zeta(p) = \sum_{n=1}^\infty n^{-p}$ to obtain $\int_0^\infty \frac{x^3}{e^x - 1} dx = \frac{4\pi}{15}$. The Debye frequency is often replaced by the *Debye temperature*

$$k_B T = \hbar\omega_d \quad (1.14)$$

so that we obtain the Debye T^3 law

$$C = Nk_B \frac{12\pi^4}{5} \frac{T^3}{(T_{Debye})^3}. \quad (1.15)$$

Debye encountered a problem that the heat capacity does not level off to $3k_B N$ at high T because his approximation allowed an infinite number of sound wave modes. To reconcile this discrepancy Debye introduced a cutoff frequency ω_{cutoff} to ensure that the number of sound wave modes is the same as the number of degrees of freedom $3N$. That is

$$\begin{aligned} 3N &= \int_0^{\omega_{\text{cutoff}}} d\omega g(\omega) \\ &= 9N \int_0^{\omega_{\text{cutoff}}} \frac{\omega^2}{\omega_d^3} d\omega \\ &= 3N \left(\frac{\omega_{\text{cutoff}}}{\omega_d} \right)^3 \end{aligned} \quad (1.16)$$

Clearly the cutoff frequency is exactly the same as the Debye frequency, i.e., $\omega_{\text{cutoff}} = \omega_d$. Note that the T^3 dependence at low temperature is still

valid even a cutoff frequency is introduced. In the high temperature limit $T \gg T_{\text{Debye}}$,

$$n_B(\beta \hbar\omega) = \frac{1}{e^{\beta \hbar\omega} - 1} \rightarrow \frac{k_B T}{\hbar\omega}, \quad (1.17)$$

and the heat capacity is

$$\begin{aligned} C &= \frac{\partial}{\partial T} \int_0^{\omega_{\text{cutoff}}} d\omega g(\omega) \hbar\omega \frac{k_B T}{\hbar\omega} \\ &= 3Nk_B. \end{aligned} \quad (1.18)$$

We then obtain the Dulong-Petit law.

shortcomings of Debye's theory

Debye's calculation successfully explains $C \sim 3Nk_B$ at high T and $C \sim T^3$ at low T . In addition, at very low temperatures, metals have a linear term in the heat capacity and the overall specific heat is $C = \gamma T + \alpha T^3$ and at low enough T the linear term dominates. Figure 1.3 shows the evidence for the existence of the linear term. As we will discuss in the next chapter, the linear dependence results from the contribution of electrons in metals.

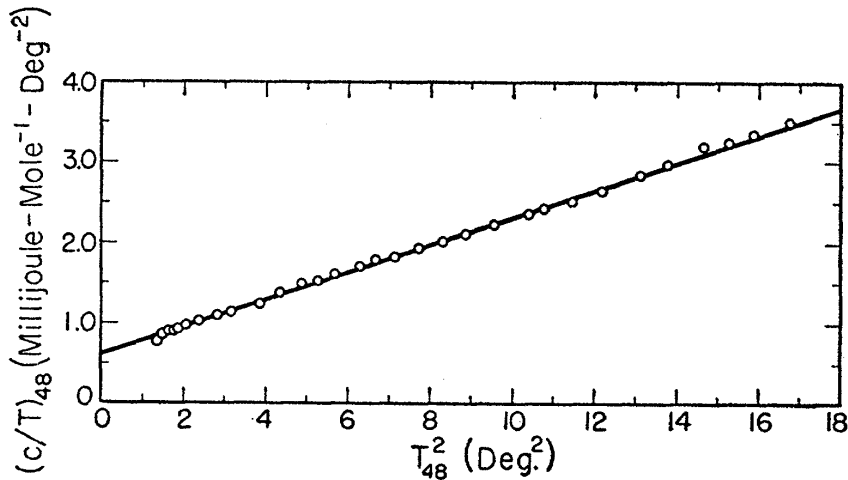


Figure 1.3: Low-T heat capacity of Ag, from Corak *et al.*, Phys. Rev. **98**, 1699 (1955).

Chapter 2

Electrons in Metals

Metals are good conductors of heat and electricity. Electrons involved with thermal and electrical conduction in metals are mobile. The conduction electrons of a metal are detached from the ionic ion and wander freely through the metal. Between collisions the interaction of a given electron, both with the others and the ions, is neglected. The neglect of electron-electron interactions between collisions is known as the *independent electron approximation*. The corresponding neglect of electron-ion interactions is known as the *free electron approximation*.

2.1 The Drude model

In 1900 Paul Drude applied Boltzmann's kinetic theory of gases to understanding electron motion within metals. The basic assumptions of the Drude model are:

- Between collisions and in the absence of external fields, conduction electrons move uniformly in a straight line. On the average, an electron travels for a time τ between two consecutive collisions. The probability of collision per unit time is $1/\tau$.
- Immediately after each collision, an electron is randomly redirected and with a speed appropriate the temperature prevailing at the place where the collision occurred. Technically one can assume that once a scattering (collision) event occurs, the electron returns to momentum $\mathbf{p} = 0$.
- Between scattering events, the electrons respond to external \mathbf{E} and \mathbf{B} fields, following Newton's law of motion.

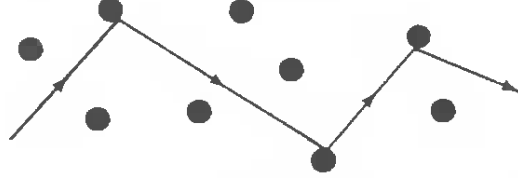


Figure 2.1: Trajectory of a conduction electron scattering off the ion according the naive picture of Drude. (from Ashcroft and Mermin's text)

Consider an electron with momentum \mathbf{p} at time t and under an externally applied force $\mathbf{F}(t)$. At time $d+dt$ the probability that the electron will scatter to $\mathbf{p} = 0$ is dt/τ , and the probability that the electron does not scatter to $\mathbf{p} = 0$ is $(1 - dt/\tau)$; the corresponding momentum change is $\mathbf{F}dt$. Combining these cases we then have

$$\mathbf{p}(t + dt) = \frac{dt}{\tau} \mathbf{0} + (1 - \frac{dt}{\tau})(\mathbf{p}(t) + \mathbf{F}dt)$$

Keeping terms only up to the linear term in dt , $d\mathbf{p} = \mathbf{F}dt - \mathbf{p}(t)dt/\tau$. Dividing this by dt and taking the limit as $dt \rightarrow 0$, we then obtain the equation of motion

$$\frac{d\mathbf{p}(t)}{dt} = \mathbf{F}(t) - \mathbf{p}(t)/\tau.$$

The effect of individual electron collisions induces a fractional damping term providing a drag force to the electron. In the absence of external field $\mathbf{F} = 0$, the electron momentum exponentially decays

$$\mathbf{p}(t) = \mathbf{p}_0 e^{-t/\tau}.$$

electrical conductivity

If electrons are under an electric field \mathbf{E} , then $\mathbf{F} = -e\mathbf{E}$ with the electron charge $-e$. In steady state $d\mathbf{p}/dt = 0$, we have

$$\mathbf{p} = m\mathbf{v} = -e\tau\mathbf{E},$$

with m the electron mass and \mathbf{v} its velocity. For electrons of density n , the electrical current is

$$\mathbf{j} = -en\mathbf{v} = \frac{e^2\tau n}{m}\mathbf{E}.$$

The electrical conductivity σ_0 , defined via $\mathbf{j} = \sigma_0\mathbf{E}$, is then

$$\sigma_0 = \frac{e^2\tau n}{m}. \quad (2.1)$$

From Eq. (2.1) we can extract the Drude scattering time to be in the range of $\tau \approx 10^{-14}$ seconds for most metals near room temperature.

Hall effect

If the system is in both an electric and a magnetic field, the equation of motion is

$$\frac{d\mathbf{p}(t)}{dt} = -e \left(\mathbf{E} + \frac{1}{c} \mathbf{v} \times \mathbf{B} \right) - \mathbf{p}/\tau. \quad (2.2)$$

For a steady state,

$$\begin{aligned} 0 &= -\mathbf{E} - \frac{1}{c} \mathbf{v} \times \mathbf{B} - \frac{m}{e\tau} \mathbf{v} \\ \mathbf{E} &= \frac{1}{nec} \mathbf{j} \times \mathbf{B} + \frac{m}{ne^2\tau} \mathbf{j}. \end{aligned} \quad (2.3)$$

The electrical conductivity and resistivity become tensors

$$\mathbf{j} = \sigma \mathbf{E} \quad \text{and} \quad \mathbf{E} = \rho \mathbf{j}.$$

The resistivity tensor is

$$\underline{\rho} = \begin{pmatrix} \rho_{xx} & \rho_{xy} & \rho_{xz} \\ \rho_{yx} & \rho_{yy} & \rho_{yz} \\ \rho_{zx} & \rho_{zy} & \rho_{zz} \end{pmatrix}, \quad \rho_{xx} = \rho_{yy} = \rho_{zz} = \frac{m}{ne^2\tau}.$$

If \mathbf{B} is oriented in the $\hat{\mathbf{z}}$ direction,

$$\underline{\rho} = \begin{pmatrix} \frac{m}{ne^2\tau} & \frac{B}{nec} & 0 \\ -\frac{B}{nec} & \frac{m}{ne^2\tau} & 0 \\ 0 & 0 & \frac{m}{ne^2\tau} \end{pmatrix}. \quad (2.4)$$

We then have

$$E_x = \frac{m}{ne^2\tau} j_x + \frac{B}{nec} j_y \quad (2.5)$$

$$E_y = -\frac{B}{nec} j_x + \frac{m}{ne^2\tau} j_y \quad (2.6)$$

Now consider an electric field is applied to a wire extending in the x -direction. The Lorentz force

$$-\frac{e}{c} \mathbf{v} \times \mathbf{B} \quad (2.7)$$

acts to deflect electrons in the negative y -direction. As the electrons accumulate at the sides of the wire, an electric field called Hall field builds up in

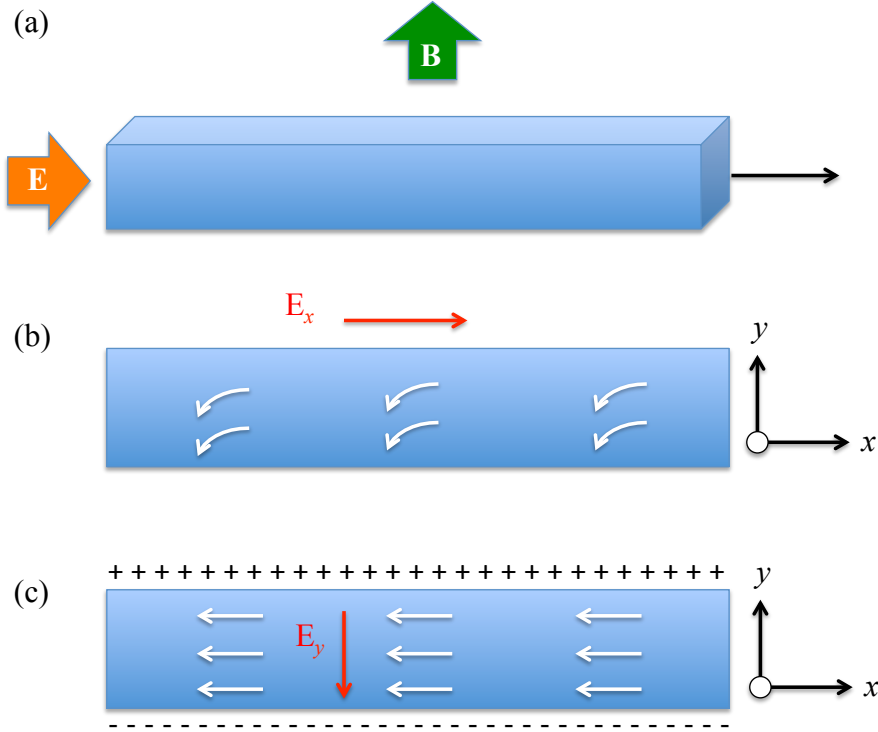


Figure 2.2: Hall effect

the y -direction. In equilibrium the Hall field will balance the Lorentz force and current will flow only in the x -direction, i.e., $j_y = 0$. The transverse Hall field E_y is proportional to B and current along the x -direction j_x . One therefore defines the Hall coefficient R_H as

$$\begin{aligned} R_H &= \frac{E_y}{j_x B} \\ &= -\frac{1}{nec}, \end{aligned} \quad (2.8)$$

which depends on no parameters of the metal except for the density of carriers. R_H is negative for free electrons. We see from the table below that for many metals this Drude theory analysis seems to make sense – the valence of Li, Na, K and also Cu are all one. However, due to "band structure" effect, the charge carriers for Be and Mg have the opposite charge from that of the electron.

Material	$(-1/[eR_H])/$ [density of atoms] In Drude theory this should give the number of free electrons per atom which is the valence	Valence
Li	.8	1
Na	1.2	1
K	1.1	1
Cu	1.5	1 (usually)
Be	-0.2	2
Mg	-0.4	2

Hall coefficients, from Simon's text

2.2 Free electron Fermi gas

For many years the electronic velocity distribution in solids was given in equilibrium at temperature T by the Maxwell-Boltzmann distribution

$$f_B(\mathbf{v}) = n \left(\frac{m}{2\pi k_B T} \right) e^{-mv^2/2\pi k_B T}.$$

In conjunction with the Drude model this leads to a wrong prediction that the contribution of an electron to the specific heat of a metal is $\frac{3}{2}k_B$. Later Sommerfeld generalized Drude's theory of metals to incorporate Fermi statistics which satisfies the Pauli exclusion principle.

Fermi-Dirac distribution

To obtain the expression of the Fermi-Dirac distribution, we begin with an N -electron system in thermal equilibrium at finite temperature.¹ The probability $P_N(\mathcal{E})$ of finding the N -particle system of energy \mathcal{E} is proportional to the Boltzmann factor $e^{-\mathcal{E}/k_B T}$, i.e.,

$$P_N(\mathcal{E}) = \frac{e^{-\mathcal{E}/k_B T}}{Z_N}, \quad Z_N = \sum_{\alpha} e^{-\mathcal{E}_{\alpha}^N/k_B T},$$

where Z_N is the partition function and is related to the Helmholtz free energy F_N as²

$$Z_N = e^{-F_N/k_B T} \tag{2.9}$$

¹The proof shown below is from Ashcroft and Mermin's text.

²For S being the entropy of the system, the Helmholtz free energy F_N is defined as $F_N \equiv \mathcal{E} - TS = -k_B T \cdot \ln Z_N$.

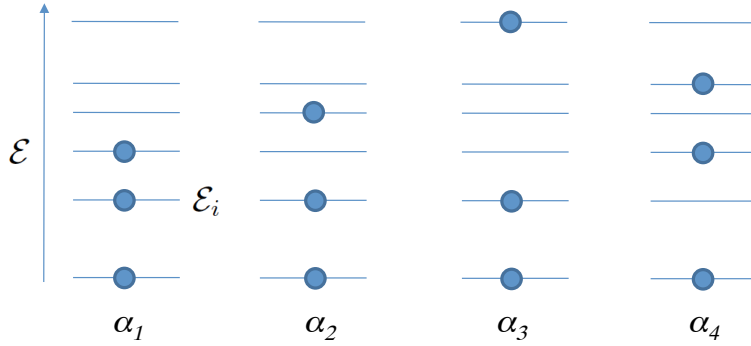


Figure 2.3: Illustration of 4 different N -electron stationary states. The filling of N one-electron states satisfies the Pauli exclusion principle. This illustration is an example of $N = 3$.

Thus the probability $P_N(\mathcal{E})$ is

$$P_N(\mathcal{E}) = e^{-(\mathcal{E} - F_N)/k_B T}. \quad (2.10)$$

Now consider a system of N electrons occupying N *one-electron states*. Assuming that the energy of an accessible N -electron state is labeled \mathcal{E}_α , the probability f_i^N of there being an electron in the i^{th} one-electron level is simply the sum of the independent probabilities $P_N(\mathcal{E}_\alpha^N)$ of finding any N -electron system in which the i^{th} electron state is occupied, i.e.,

$$f_i^N = \sum_{\alpha} P_N(\mathcal{E}_\alpha^N) = \sum_{\alpha} e^{-(\mathcal{E}_\alpha^N - F_N)/k_B T}, \quad (2.11)$$

where the summation is over all N -electron states α .

The expression of f_i^N can be obtained through the following three steps.

1. The Pauli exclusion principle requires that any one-electron state is either occupied or unoccupied. If the probability of finding an N -electron state in which no electron being in the i^{th} one-electron state is $P_N(\mathcal{E}_\gamma^N)$, we could equally well write Eq. 2.12 as³

$$f_i^N = 1 - \sum_{\gamma} P_N(\mathcal{E}_\gamma^N) \quad (2.12)$$

³The Pauli exclusion principle requires $\sum_{\alpha} P_N(\mathcal{E}_\alpha^N) + \sum_{\gamma} P_N(\mathcal{E}_\gamma^N) = 1$

2. An N -electron state in which there is no electron in the one-electron state i of energy ε_i can be constructed by removing the electron in the i^{th} one-electron state of any $(N+1)$ -electron state in which there is an electron in the i^{th} one-electron state, i.e.,

$$f_i^N = 1 - \sum_{\alpha} P_N(\mathcal{E}_{\alpha}^{N+1} - \varepsilon_i). \quad (2.13)$$

Using Eqs. 2.10, we have

$$\begin{aligned} P_N(\mathcal{E}_{\alpha}^{N+1} - \varepsilon_i) &= e^{-(\mathcal{E}_{\alpha}^{N+1} - \varepsilon_i - F_N)/k_B T} \\ &= e^{(\varepsilon_i - F_{N+1} + F_N)/k_B T} e^{-(\mathcal{E}_{\alpha}^{N+1} - F_{N+1})/k_B T} \\ &= e^{(\varepsilon_i - \mu)/k_B T} P_{N+1}(\mathcal{E}_{\alpha}^{N+1}), \end{aligned} \quad (2.14)$$

where $\mu = F_{N+1} - F_N$ is known as the chemical potential. Therefore we could rewrite Eq. 2.13 as

$$f_i^N = 1 - e^{(\varepsilon_i - \mu)/k_B T} \sum_{\alpha} P_{N+1}(\mathcal{E}_{\alpha}^{N+1}) = 1 - e^{(\varepsilon_i - \mu)/k_B T} f_i^{N+1}, \quad (2.15)$$

3. When N is very large (of the order of 10^{23}), f_i^{N+1} can be replaced by f_i^N , giving rise to

$$f_i^N = \frac{1}{e^{(\varepsilon_i - \mu)/k_B T} + 1} \quad (2.16)$$

Now we have proved the Fermi-Dirac distribution. In summary, given a system of free electrons with chemical potential μ , the probability of an eigenstate of energy \mathcal{E} being occupied is given the Fermi function

$$f(\varepsilon, \mu, T) = \frac{1}{e^{(\varepsilon - \mu)/k_B T} + 1}. \quad (2.17)$$

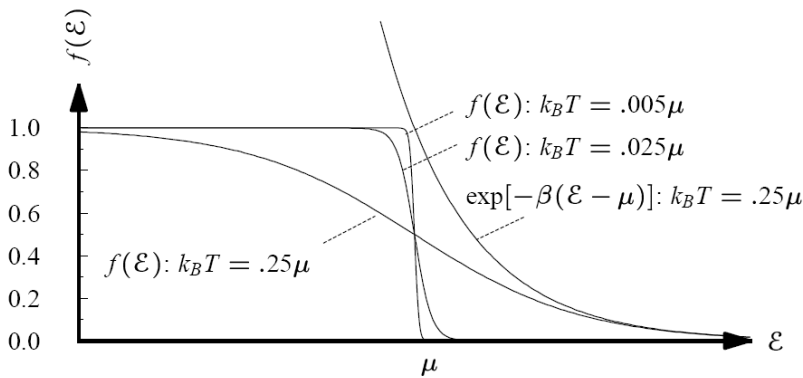


Figure 2.4: Sketch of the Fermi function for various values of $k_B T$, from Marder's text.

At $T = 0$ the Fermi function becomes a step function and the chemical potential defined is the *Fermi energy*. States below the chemical potential are filled and those above the chemical potential are empty, whereas at higher temperatures the Fermi function become more smeared out. For materials with an energy gap, the chemical potential is precisely halfway between the highest-energy filled eigenstate and

The free electron model

Much of solid-state physics is determined by the Hamiltonian of the system

$$\hat{\mathcal{H}} = \sum_{l=1}^N \frac{\hat{P}_l}{2m_l} + \frac{1}{2} \sum_{l \neq l'} \frac{q_l q_{l'}}{|\mathbf{r}_l - \mathbf{r}_{l'}|}. \quad (2.18)$$

The summation runs over all electrons and nuclei of charge q_l at position \mathbf{r}_l in solids. However, it can't be solved without approximations because of the enormous number of particles in actual solids. The simplest approximation is the *free electron gas model* which assumes that a set of "noninteracting" electrons freely move about, subject only to the Pauli exclusion principle – no two electrons occupy the same quantum mechanical state. Since electrons are assumed to have no interactions, the one-electron wave function associated with an energy level ε satisfies

$$-\frac{\hbar^2}{2m} \nabla^2 \psi(\mathbf{r}) = \varepsilon \psi(\mathbf{r}). \quad (2.19)$$

The eigenfunction of a many-electron system is simply the product of the one-electron wave functions. The energy of the many-electron system is the sum of all one-electron energies. Assume that electrons are confined in a square box of side length L , $L^3 = V$. We then have the boundary Born-von Karman condition

$$\begin{aligned} \psi(x + L, y, z) &= \psi(x, y, z), \\ \psi(x, y + L, z) &= \psi(x, y, z), \\ \psi(x, y, z + L) &= \psi(x, y, z). \end{aligned} \quad (2.20)$$

The eigenfunction of the Schrödinger equation Eq. 2.19 is

$$\psi_{\mathbf{k}}(\mathbf{r}) = \frac{1}{\sqrt{V}} e^{i\mathbf{k}\cdot\mathbf{r}}, \quad (2.21)$$

with energy

$$\varepsilon(\mathbf{k}) = \frac{\hbar^2 k^2}{2m}. \quad (2.22)$$

Now we invoke the boundary condition Eq. 2.20 and obtain

$$e^{ik_x L} = e^{ik_y L} = e^{ik_z L} = 1. \quad (2.23)$$

This permits certain discrete values of \mathbf{k} . Thus in a 3D space with Cartesian axes k_x, k_y and k_z (known as k -space), the allowed \mathbf{k} 's are those whose coordinates along the three axes are given by integral multiples of $2\pi/L$. The wave vector \mathbf{k} must be of the form

$$\mathbf{k} = (k_x, k_y, k_z) = (n_x, n_y, n_z) \frac{2\pi}{L}, \quad (2.24)$$

with n_x, n_y, n_z integers. In k -space, if there is a very large number of states, the volume of each k point is $(2\pi/L)^3$. Therefore a region of k -space of volume Ω will contain

$$\frac{\Omega}{(2\pi/L)^3} = \frac{\Omega V}{8\pi^3} \quad (2.25)$$

allowed value of \mathbf{k} . The k -space density of states per unit volume is $1/8\pi^3$.

In building up the N -electron ground state, we begin with by placing "two" electrons in the one-electron level $\mathbf{k} = 0$ for spin up and spin down, which has the lowest possible one-electron energy $\varepsilon = 0$. We then continue to add electrons, successively filling the one-electron levels of lowest energy that are not already occupied. Since ε is proportional to k^2 and $N \gg 1$, the occupied region will be distinguishable from a sphere (*the Fermi sphere*) with a radius called k_F (*the Fermi wave vector*) and its volume is $\Omega = 4\pi k_F^3/3$. The surface of the Fermi sphere is known as the *Fermi surface*, the energy surface in k -space dividing filled from unfilled states at zero temperature. The total number of electrons is

$$N = 2 \left(\frac{4\pi k_F^3}{3} \right) \left(\frac{V}{8\pi^3} \right) = \frac{k_F^3}{3\pi^2} V \quad (2.26)$$

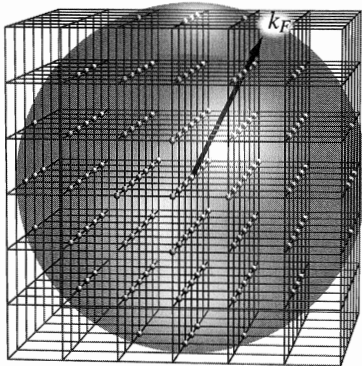


Figure 2.5: The ground state of the free electron gas is constructed by occupying a sphere of states in k -space, whose radius is k_F . (from Marder's text)

and the electron density

$$n = \frac{N}{V} = \frac{k_F^3}{3\pi^2}, \quad (2.27)$$

i.e., $k_F = (3\pi^2 n)^{1/3}$. Since $mv = \hbar k$, we then have the *Fermi velocity*

$$v_F = \frac{\hbar k_F}{m} = \frac{\hbar(3\pi^2 n)^{1/3}}{m}. \quad (2.28)$$

In addition, for a metal, the Fermi energy is the highest occupied one-electron energy

$$\begin{aligned} \varepsilon_F &= \frac{\hbar^2 k_F^2}{2m} \\ &= \frac{\hbar^2 (3\pi^2 n)^{2/3}}{2m}. \end{aligned} \quad (2.29)$$

2.3 Electronic Heat Capacity

To calculate the heat capacity of electrons in a metal, we first find out the temperature dependence of the total electronic energy by using the Fermi function. The total energy is

$$\mathcal{E}_{\text{total}} = 2 \sum \varepsilon(\mathbf{k}) f(\varepsilon, \mu, T) \quad (2.30)$$

Replacing the summation by $\frac{V}{(2\pi)^3} \int d\mathbf{k}$,

$$\begin{aligned} \mathcal{E}_{\text{total}} &= \frac{2V}{(2\pi)^3} \int \varepsilon(\mathbf{k}) f(\varepsilon, \mu, T) d\mathbf{k} \\ &= \frac{2V}{(2\pi)^3} 4\pi \int_0^\infty k^2 \varepsilon(\mathbf{k}) f(\varepsilon, \mu, T) dk, \end{aligned}$$

where the chemical potential is defined by

$$N = \frac{2V}{(2\pi)^3} 4\pi \int_0^\infty k^2 f(\varepsilon, \mu, T) dk.$$

Because $k = \sqrt{2\varepsilon m / \hbar^2}$, we have

$$\int dk = \int \sqrt{\frac{m}{2\varepsilon \hbar^2}} d\varepsilon,$$

and

$$\begin{aligned}\mathcal{E}_{\text{total}} &= \frac{2V}{(2\pi)^3} 4\pi \int_0^\infty \frac{2m\varepsilon}{\hbar^2} \varepsilon f(\varepsilon, \mu, T) \sqrt{\frac{m}{2\varepsilon\hbar^2}} d\varepsilon, \\ &= V \int_0^\infty \frac{(2m)^{3/2}}{2\pi^2\hbar} \sqrt{\varepsilon} f(\varepsilon, \mu, T) \varepsilon d\varepsilon, \\ &= V \int_0^\infty g(\varepsilon) f(\varepsilon, \mu, T) \varepsilon d\varepsilon,\end{aligned}$$

where

$$g(\varepsilon) = \frac{(2m)^{3/2}}{2\pi^2\hbar^3} \sqrt{\varepsilon} \quad (2.31)$$

is the *density of states per unit volume*, giving the number of eigenstates (including both spin states) with energies between ε and $\varepsilon + d\varepsilon$. Note that the density of states can also be expressed as

$$g(\varepsilon) = \frac{3n}{2\varepsilon_F} \sqrt{\frac{\varepsilon}{\varepsilon_F}}, \quad (2.32)$$

because

$$\varepsilon_F = \frac{\hbar^2(3\pi^2n)^{2/3}}{2m}. \quad (2.33)$$

Similarly the total number of states is

$$N = V \int_0^\infty g(\varepsilon) f(\varepsilon, \mu, T) d\varepsilon.$$

Now we calculate the increase ΔU in the total energy for $k_B T \ll \varepsilon_F$. The energy increase of an N -electron system when heated from 0 to T is

$$\begin{aligned}\Delta U &= U(T) - U(0) \\ &= V \int_0^\infty g(\varepsilon) f(\varepsilon, \mu, T) \varepsilon d\varepsilon - V \int_0^{\varepsilon_F} g(\varepsilon) \varepsilon d\varepsilon,\end{aligned} \quad (2.34)$$

since the Fermi function $f(\varepsilon, \mu, T)$ is a step function at $T=0$. In addition, the total number of electron is conserved during the change of temperature, i.e., $N(T) = N(T = 0)$. We obtain the identity

$$\varepsilon_F \int_0^\infty g(\varepsilon) f(\varepsilon, \mu, T) d\varepsilon = \varepsilon_F \int_0^{\varepsilon_F} g(\varepsilon) d\varepsilon.$$

With this identify, Eq. 2.34 can be rewritten as

$$\Delta U = V \int_0^\infty g(\varepsilon) f(\varepsilon, \mu, T) (\varepsilon - \varepsilon_F) d\varepsilon - V \int_0^{\varepsilon_F} g(\varepsilon) (\varepsilon - \varepsilon_F) d\varepsilon. \quad (2.35)$$

The next step is to find $\partial U / \partial T$. The only temperature-dependent term in Eq. 2.35 is $f(\varepsilon, \mu, T)$, so the heat capacity is

$$C = \frac{dU}{dT} = V \int_0^\infty g(\varepsilon) \frac{df(\varepsilon, \mu, T)}{dT} (\varepsilon - \varepsilon_F) d\varepsilon.$$

For low temperature, f is a step-like function and df/dT is large only at energies near ε_F . A good approximation to the calculation of heat capacity is to replace μ and $g(\varepsilon)$ in the integrand by ε_F and $g(\varepsilon_F)$, respectively, and take $g(\varepsilon_F)$ outside of the integral, i.e.,

$$C = Vg(\varepsilon_F) \int_0^\infty d\varepsilon \frac{df}{dT} (\varepsilon - \varepsilon_F).$$

Note that

$$\frac{df(\varepsilon - \varepsilon_F)}{dT} = \frac{\varepsilon - \varepsilon_F}{k_B T^2} \frac{e^{(\varepsilon - \varepsilon_F)/k_B T}}{(e^{(\varepsilon - \varepsilon_F)/k_B T} + 1)^2} \quad (2.36)$$

We then have

$$C = Vg(\varepsilon_F) k_B^2 T \int_{-\varepsilon_F/k_B T}^\infty dx \frac{x^2 e^x}{(e^x + 1)^2} \quad (2.37)$$

From Eq. (2.32) we know that $g(\varepsilon_F) = 3n/2\varepsilon_F$, so⁴

$$\begin{aligned} C &\approx \frac{3N}{2\varepsilon_F} k_B^2 T \int_{-\infty}^\infty dx \frac{x^2 e^x}{(e^x + 1)^2} \\ &= \frac{\pi^2 N k_B}{2} \frac{k_B T}{\varepsilon_F} \end{aligned} \quad (2.38)$$

2.4 Thermionic Emission of Electrons from Metals

⁴ $\int_{-\infty}^\infty dx \frac{x^2 e^x}{(e^x + 1)^2} = \frac{\pi^2}{3}$

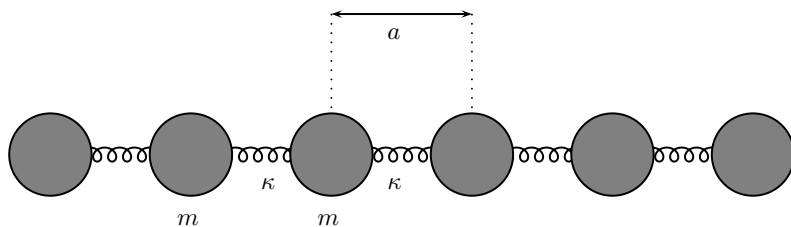
Chapter 3

Vibrations of One-Dimensional Lattices

In the first two chapters we discuss the thermal properties of solids without considering their microstructure seriously. Our simple models of solids, and electrons in solids, are insufficient for correctly understanding the physics of solids. In order to improve our understanding, we now take the periodic crystal structures into account. To get a qualitative understanding of the effects of the periodic lattice, we start with simple one dimensional systems. We will be able to better understand the shortcomings of Einstein and Debye models of vibrations in solids.

3.1 One-dimensional monatomic solids

For simplicity, let's imagine a *true* one-dimensional system of atoms of mass m where there is only the longitudinal motion and the equilibrium spacing between atoms is a . Define the position of the n^{th} atom to be x_n and the equilibrium position of the n^{th} atom to be $x_n^{\text{eq}} = na$. The Taylor



expansion of the potential $V(x)$ between the atoms around its minimum is

$$V(x) \approx V(x^{\text{eq}}) + \frac{\kappa}{2}(x - x^{\text{eq}})^2 + \frac{\kappa_3}{3!}(x - x^{\text{eq}})^3 + \dots$$

In addition, atoms move with their position deviating from their equilibrium position by

$$\delta x_n = x_n - x_n^{\text{eq}}.$$

With this quadratic interatomic potential, we can write the total potential energy of the chain to be

$$V_{\text{tot}} = V_{\text{eq}} + \sum_i V(x_{i+1} - x_i) = V_{\text{eq}} + \sum_i \frac{\kappa}{2}(\delta x_{i+1} - \delta x_i)^2.$$

The force on the n^{th} mass on the chain is then given by

$$F_n = -\frac{\partial V_{\text{tot}}}{\partial x_n} = \kappa(\delta x_{n+1} - \delta x_n) + \kappa(\delta x_{n-1} - \delta x_n).$$

Thus we have the equation of motion

$$m(\delta \ddot{x}) = F_n = \kappa(\delta x_{n+1} + \delta x_{n-1} - 2\delta x_n)$$

Note that, for any coupled system system, a *normal mode* is defined to be a collective oscillation where all particles move at the same frequency. We now find solutions to the equation of motion by using a trial solution (*ansatz*) that describes the normal modes as waves

$$\delta x_n = A e^{i\omega t - ikx_n^{\text{eq}}} = A e^{i\omega t - ikna}. \quad (3.1)$$

Plugging the ansatz into the equation of motion, we obtain

$$-m\omega^2 A e^{i\omega t - ikna} = \kappa A e^{i\omega t} [e^{-ika(n+1)} + e^{-ika(n-1)} - 2e^{-ikan}],$$

i.e.,

$$m\omega^2 = 2\kappa[1 - \cos(ka)] = 4\kappa \sin^2(ka/2).$$

Therefore the *dispersion relation* between frequency ω and wave vector k is

$$\omega = 2\sqrt{\frac{\kappa}{m}} \left| \sin\left(\frac{ka}{2}\right) \right|. \quad (3.2)$$

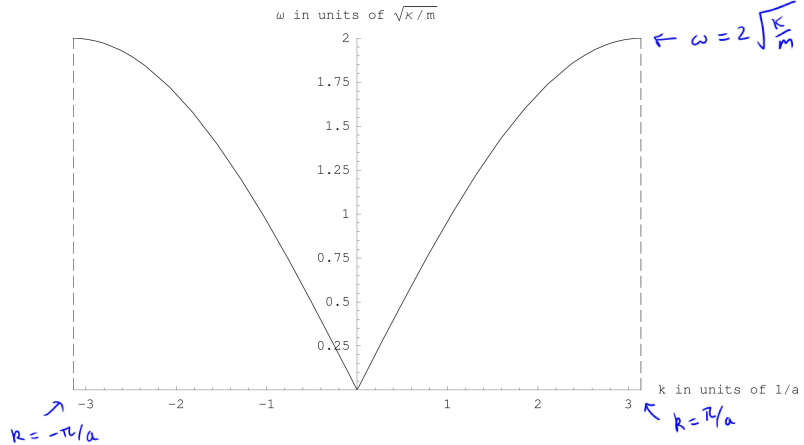


Figure 3.1: Dispersion relation between ω and k for $-\frac{\pi}{a} \leq k \leq \frac{\pi}{a}$

3.2 Reciprocal lattice

Figure 3.1 plots the ω vs. k dispersion relation for $-\frac{\pi}{a} \leq k \leq \frac{\pi}{a}$ because the system is periodic in real space with a periodicity a , corresponding to a reciprocal space (k space) with periodicity $\frac{2\pi}{a}$. It is obvious that the energy and wave functions of vibrations are invariant under a $k \rightarrow k + \frac{2\pi}{a}$ translation in reciprocal space, because

$$e^{-i2\pi n} = 1$$

and

$$\delta x_n = A e^{i\omega t - i(k+2\pi/a)na} = A e^{i\omega t - ikna}.$$

In fact if we shift k by any vector $\frac{2\pi}{a}p$ with p an integer, we will have exactly the same wave as well. Therefore $\frac{2\pi}{a}m$ in k -space (reciprocal space) with m an integer are all physically equivalent to the point $k = 0$. This result is quite profound. One must notice the statement that k and $k + \frac{2\pi}{a}m$ are equivalent in describing lattice vibrations is valid ONLY if one measures the wave at lattice point $x_n = na$ and not at arbitrary points x along the axis. This phenomenon, that two waves with different wavelengths will appear the same if they are sampled only the lattice points, is known as *aliasing* of waves. See Fig. 3.2. If the physical waves is only defined at lattice points, the two waves are fully equivalent.

A set of points $G_m = \frac{2\pi}{a}m$ are defined as *reciprocal lattice*, corresponding to the *real-space lattice* of lattice constant a , the original periodic set of points

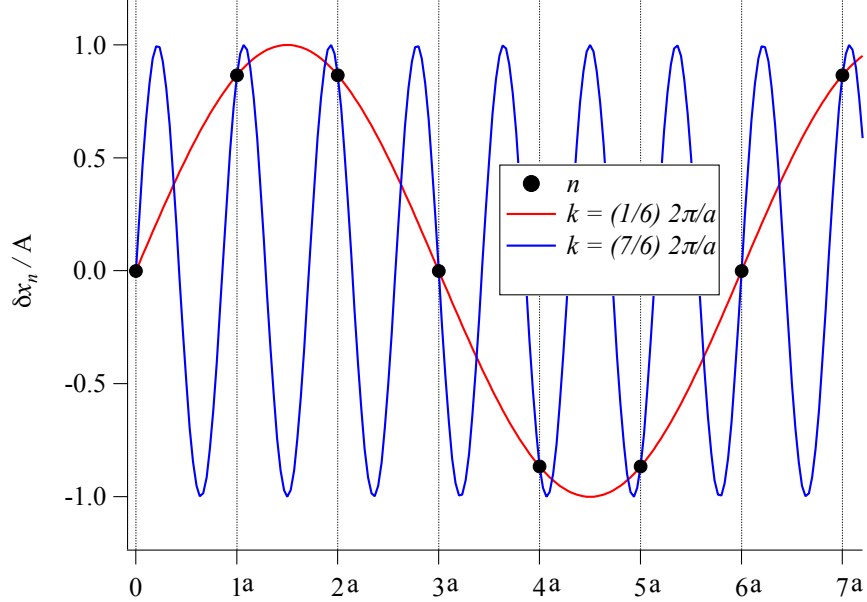


Figure 3.2: Plot of atom displacements δx versus position x . These displacements are described equally well by $e^{i\omega t - ikx}$ and $e^{i\omega t - i(k + \frac{2\pi}{a})x}$ for $x = na$. Here $k = \frac{\pi}{3a}$.

$x_n = na$, i.e.,

$$\text{real-spacelattice } x_n = \dots -2a, -a, 0, a, 2a, \dots$$

$$\text{reciprocal lattice } G_n = \dots -2\left(\frac{2\pi}{a}\right), -\left(\frac{2\pi}{a}\right), 0, \left(\frac{2\pi}{a}\right), 2\left(\frac{2\pi}{a}\right)$$

One important property of the reciprocal lattice points G_m and the real-space lattice points x_n is

$$e^{iG_m x_n} = 1. \quad (3.3)$$

We also have the following terminologies:

- *Brillouin Zone*: the periodic unit (the unit cell) in k -space.
- *First Brillouin Zone*: a unit cell in k -space centered around the point $k = 0$, i.e., $-\pi/a \leq k < \pi/a$
- *Brillouin-Zone boundary*: $k = \pm\pi/a$, points which are symmetric around $k = 0$ and are separated by $2\pi/a$.

Sound waves

In the acoustic branch, the frequency is linearly proportional to wave vector in the small k regime (long wavelength)

$$\omega = \sqrt{\frac{\kappa}{m}} ka.$$

Sound wave is a vibration of long wavelength, and its velocity is $\sqrt{\frac{\kappa}{m}}a$. In contrast, the dispersion is no longer linear at large k . This is in disagreement with what was assumed in Debye's model. At large k , the group velocity $d\omega/dk$, the speed at which a wavepacket moves, differs from the phase velocity ω/k .

At the zone boundary $k = \pm\pi/a$, the displacement $\Re[\delta x_n]$ at time t is described as

$$\Re[\delta x_n] = \Re[Ae^{i\omega t - ikna}] = A(-1)^n \cos \omega t, \quad (3.4)$$

so the alternate atoms oscillate in opposite phases. This is consistent with that the group velocity becomes zero at the Brillouin zone boundaries $k = \pm\pi/a$ (i.e., the dispersion is flat), implying that no energy is propagated. In other words a sound wave whose wavelength is twice the lattice spacing, i.e., $\lambda = 2a$, will experience reflection from the periodic array of atoms, so that the sound wave becomes a standing wave made up of two waves going in opposite directions.

Number of normal modes

Assume that there are exactly N atoms and use the Born-von Barman periodic boundary condition $e^{ikNa} = 1$, This requirement restricts the possible values of k to be of the form

$$k = \frac{2\pi p}{Na} = \frac{2\pi p}{L}.$$

where p is an integer and L is the total length of the system. Thus k becomes discrete rather than a continuous variable; the spacing between two of these consecutive points being $2/Na$,

$$k = \frac{2\pi p}{Na} = \frac{2\pi p}{L}.$$

Thus the total number of normal modes is

$$\frac{\text{Range of } k \text{ the 1st BZ}}{\text{space between neighboring}} = \frac{2\pi/a}{2\pi/Na} = N.$$

As insightfully predicted by Debye in order to cut off his divergent integrals in calculating heat capacity, there is precisely one normal mode per degree of freedom in the whole system.

3.3 Diaomic chain

Consider a model of periodic arrangement of two different types of atoms with masses m_1 and m_2 . The springs connecting the atoms have spring constants κ_1 and κ_2 also alternate. We assume that $m_1 = m_2$ and identify a unit cell with a length a known as the lattice constant. Note that the definition of the unit cell is extremely non-unique.¹ We could just as well have chosen (for example) the unit cell shown by the box of dotted line in Fig. 3.4. One can pick some reference point inside each unit cell to define a lattice. We can set the reference lattice point r_n in unit cell n as

$$r_n = na.$$

Analogous to the case of monoatomic chain, we can have the equations of motion for a diatomic chain

$$\begin{aligned} m(\delta\ddot{x}_n) &= \kappa_2(\delta y_n - \delta x_n) + \kappa_1(\delta y_{n-1} - \delta x_n) \\ m(\delta\ddot{y}_n) &= \kappa_1(\delta x_{n+1} - \delta y_n) + \kappa_2(\delta x_n - \delta y_n), \end{aligned} \quad (3.5)$$

where δx_n and δy_n are displacements of atoms #1 and #2 in the unit cell, respectively. For trial solutions

$$\delta x_n = A_x e^{i\omega t - ikna} \quad \text{and} \quad \delta y_n = A_y e^{i\omega t - ikna},$$

¹A unit cell is the repeated pattern which is the elementary building block of a periodic crystal.

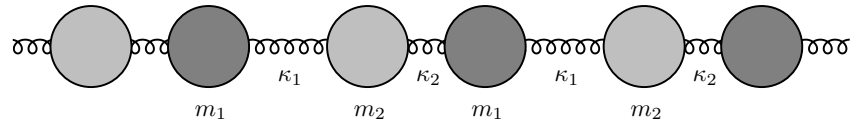


Figure 3.3: Diatomic chain structure.

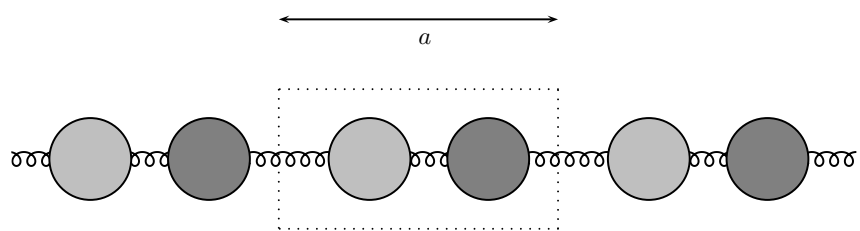


Figure 3.4: Diatomic chain structure with a unit cell

it is straightforward to obtain

$$m\omega^2 \begin{pmatrix} A_x \\ A_y \end{pmatrix} = \begin{pmatrix} \kappa_1 + \kappa_2 & -\kappa_1 e^{ika} - \kappa_2 \\ -\kappa_1 e^{ika} - \kappa_2 & \kappa_1 + \kappa_2 \end{pmatrix} \begin{pmatrix} A_x \\ A_y \end{pmatrix}.$$

So the dispersion is

$$\omega_{\pm} = \sqrt{\frac{\kappa_1 + \kappa_2}{m}} \pm \frac{1}{m} \sqrt{\kappa_1^2 + \kappa_2^2 + 2\kappa_1\kappa_2 \cos(ka)}. \quad (3.6)$$

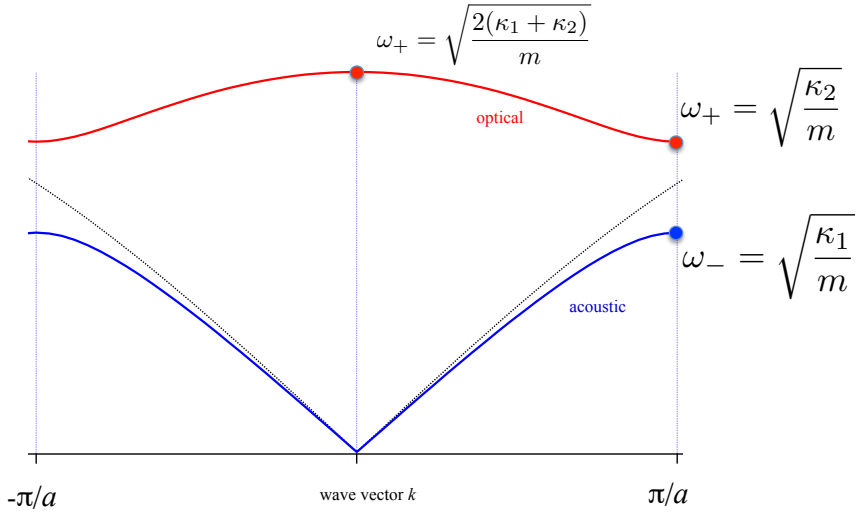


Figure 3.5: Dispersion of a diatomic chain.

Figure 3.5 plots the ω -vs.- k dispersion for the lattice vibration of this diatomic chain system. There are two modes,² acoustic mode (ω_-) and optical mode (ω_+), in the dispersion. The definition of an *acoustic mode* is any mode that has linear dispersion as $k \rightarrow 0$. For small k , the frequency of acoustic phonons is³

$$\omega_- \approx \sqrt{\frac{\kappa_1\kappa_2}{2m(\kappa_1 + \kappa_2)}} ka$$

and the sound velocity is

$$v_{\text{sound}} = \sqrt{\frac{a^2\kappa_1\kappa_2}{2m(\kappa_1 + \kappa_2)}}. \quad (3.7)$$

²In three dimension, if there are n atoms per unit cell, there will be $3(n - 1)$ optical modes but always 3 acoustic modes.

³Use $\cos x \approx 1 - \frac{x^2}{2}$ for $x \ll 1$.

In addition, as $k \rightarrow 0$, the eigenvalue equation Eq. 3.6 takes the simple form

$$\omega^2 \begin{pmatrix} A_x \\ A_y \end{pmatrix} = \frac{\kappa_1 + \kappa_2}{m} \begin{pmatrix} 1 & -1 \\ -1 & 1 \end{pmatrix} \begin{pmatrix} A_x \\ A_y \end{pmatrix}.$$

Therefore the acoustic mode has a zero frequency at $k = 0$ and its eigenvector, i.e., amplitude, is

$$\begin{pmatrix} A_x \\ A_y \end{pmatrix} = \begin{pmatrix} 1 \\ 1 \end{pmatrix},$$

implying that both atoms in the unit cell move together in the same direction as depicted in Fig. 3.6.

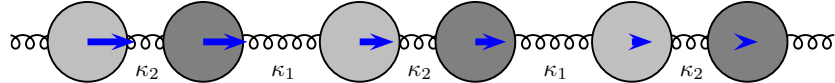


Figure 3.6: A long wavelength acoustic mode.

For the optical mode, its frequency goes to $\sqrt{2(\kappa_1 + \kappa_2)/m}$ at $k = 0$, and its eigenvector is

$$\begin{pmatrix} A_x \\ A_y \end{pmatrix} = \begin{pmatrix} 1 \\ -1 \end{pmatrix}.$$

Fig. 3.7 shows that both masses in the unit cell move in the same direction.

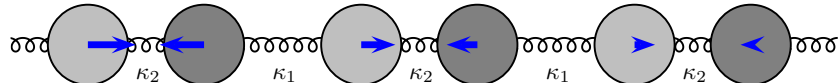


Figure 3.7: A long wavelength optical mode.

3.4 Quantized waves: phonons

Einstein used the concept of harmonic oscillator to calculate the heat capacity of solids with a fixed frequency, Einstein frequency. Debye extended his idea with frequency $\omega = vk$.

The dynamics of the lattice is governed by the classical Hamiltonian: $H = P^2/2m + V$

From the viewpoint of quantum mechanics, those waves become quantized with energy

$$\varepsilon = \hbar\omega \left(n + \frac{1}{2} \right). \quad (3.8)$$

Analogous to defining a single quantum of light as a photon, the quantum of energy of lattice vibration is called *phonon*. Characteristics of phonons are summarized below:

1. Both phonons and photons are bosons and are categorized as *quasiparticle*⁴.
2. In the energy expression Eq. 3.8 of phonon, the energy level is occupied by n phonons of energy $\hbar\omega$; $\frac{1}{2}\hbar\omega$ is the zero-point energy. The existence of zero-point energy supports Heisenberg's uncertainty principle.
3. The occupation number is temperature dependent

$$n_B(\omega, T) = \frac{1}{e^{\hbar\omega/K_B T} - 1}. \quad (3.9)$$

4. A phonon can interact with other particles such as photons, neutrons, electrons and so on, as it has a momentum which is the momentum modulo the reciprocal lattice. In other words, the wave vector k of phonons must be within the first Brillouin zone and $\hbar k$ is known as the *crystal momentum*.

The total vibration energy⁵

$$U_{\text{tot}} = \frac{Na}{2\pi} \int_{-\pi/a}^{\pi/a} dk \hbar\omega(k) \left(n_B(k) + \frac{1}{2} \right), \quad (3.10)$$

from which we could calculate the heat capacity as dU/dT . This is a 1D version of Eq. 1.9. In comparison with Einstein and Debye models, the frequency dispersion is no longer linear in the 1D-monoatomic-chain model discussed here and we, instead of using a cutoff frequency, use the continuum integral to count the total number of phonon modes,

$$\left(\int_{-\pi/a}^{\pi/a} dk \right) / \frac{2\pi}{Na} = N. \quad (3.11)$$

⁴A quasiparticle is

⁵Using $\sum_k \rightarrow \frac{Na}{2\pi} \int dk$

Although the linear dispersion is invalid, it is useful to further replace integrals over k with integrals over frequency to obtain density of states $g(\omega)$

$$\frac{2\pi}{Na} \int_{-\pi/a}^{\pi/a} dk = \int d\omega g(\omega), \quad (3.12)$$

where

$$g(\omega) = \frac{Na}{\pi} \left| \frac{dk}{d\omega} \right|. \quad (3.13)$$

3.5 Thermal expansion

3.6 Heat conduction by phonons

Chapter 4

Crystal structure

After learning some macroscopic properties of solids, we need to understand their atomic arrangements for further studies of the rich physics of solids. For almost all the elements and for a vast array of compounds, the lowest-energy state is crystalline. Crystalline order is the simplest way that atoms could be possibly be arranged to form a macroscopic solid. We here survey some of the most important geometrical properties of periodic arrays in three dimensional space.

4.1 Lattices and unit cells

Lattices

A *lattice* is a set of points where the environment of any given point is equivalent to the environment of any other given point. Mathematically this set of points \mathbf{R} is defined by integer sums of a set of linearly independent primitive basis vectors \mathbf{a}_i with $i = 1, 2$, and 3 ,

$$\mathbf{R} = n_1 \mathbf{a}_1 + n_2 \mathbf{a}_2 + n_3 \mathbf{a}_3, \quad (4.1)$$

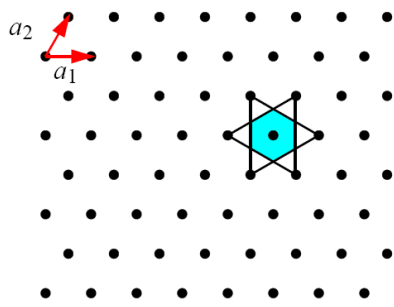


Figure 4.1: A hexagonal lattice, also called a triangular lattice, is symmetric under reflection about x & y axes, and 60° -rotation, from Marder's text

where n_i are integers. The choice of primitive basis vectors is not unique. One should note that not all periodic arrangements of points are lattices. For example a 2D honeycomb shown in Fig. 4.2 is not a lattice. The environment of point P and point R are actually different – point P has a neighbor directly above it (the point R), whereas point R has no neighbor directly above. Nevertheless all equivalent points form a triangular lattice, as demonstrated in Fig. 4.3.

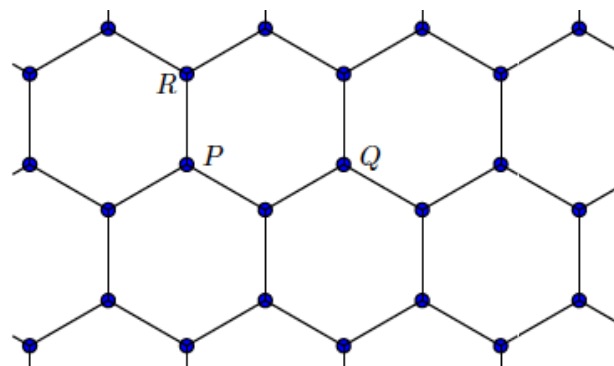


Figure 4.2: The honeycomb is not a lattice. Points P and R are inequivalent. (Points P and Q are equivalent), from Simon's text

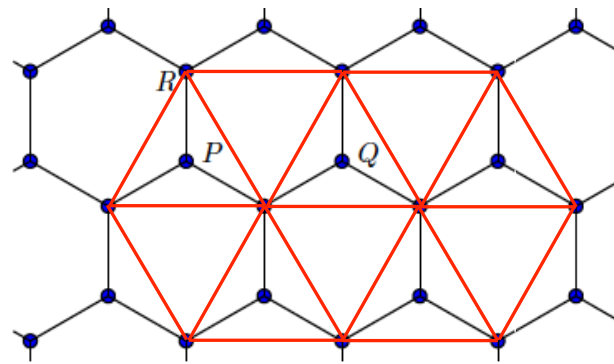


Figure 4.3: The honeycomb is not a lattice, but all equivalent points form a triangular lattice.

Unit cells

A *unit cell* is a region of space, such that when many identical units are stacked together it completely fills all of space and reconstructs the full structure. Because lattices are created by repeating basic units over and over throughout space, the full information of a crystal can be obtained in a small region of space. Such a region, chosen to be as small as it can be, is called *primitive unit cell*. In other words, a primitive cell is a volume of space that, when translated through all the vectors in a lattice, just fills all of space without either overlapping itself or leaving voids. So a primitive unit cell for a periodic crystal is a unit cell containing only a single lattice point.

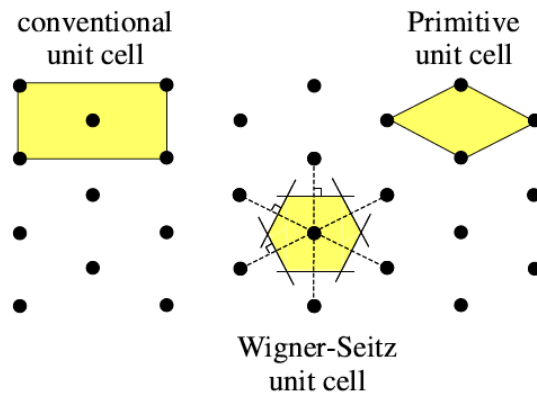


Figure 4.4: Some unit cells for the triangular lattice, from Simon's text.

One can also fill space up with nonprimitive cells (known as conventional cells). The conventional unit cell is a region that just fills space without any overlapping when translated through some subset of the vectors of a lattice. The conventional unit cell is generally chosen to be bigger than a primitive cell and to have the required symmetry. The *Wigner-Seitz cell* about a lattice point is the region of space that is closer to any other lattice point. The Wigner-Seitz cell is a primitive cell with full symmetry of the lattice. One way to construct the Wigner-Seitz cell is to draw the perpendicular bisector of all the lines between a lattice point to each of its neighbor.

4.2 Symmetry of 3D crystals

The set of points specified in Eq. 4.1 is often called the Bravais lattice. From the viewpoint of symmetry, a Bravais lattice is characterized by the

specification of all rigid body operations that take the lattice to itself. This set of operations is known as the *symmetry group* or *space group* of the Bravais lattice. The operations in the symmetry group include all translations through lattice vectors. In addition, there will be rotations, reflections, and inversions that take the lattice to itself. For example, a simple hexagonal lattice is taken to itself by a rotation through 60° about a line of lattice point parallel to the c -axis, and reflection in the lattice plane perpendicular to the c -axis.

Any symmetry operation of a Bravais lattice can be combined out of a translation $T_{\mathbf{R}}$ through a lattice vector \mathbf{R} and rigid body operation leaving at least one lattice point fixed. The *point group* of a lattice is defined as a subset of the full symmetry group which leaves a particular point fixed. There are only 7 distinct point group that a Bravais lattice can have, so there are 7 three-dimensional crystal systems. When the full symmetry is considered, there are 14 distinct space groups that a Bravais lattice can have. Thus, from the view of point of symmetry, there are 14 different kinds of Bravais lattice.¹ The general one is the triclinic lattice. The general triclinic lattice is a unit cell, which is a parallelepiped with all sides different lengths, and all angle different from 90° or 120° . The other 13 lattices have some symmetry, such as relations between the sides or angles.

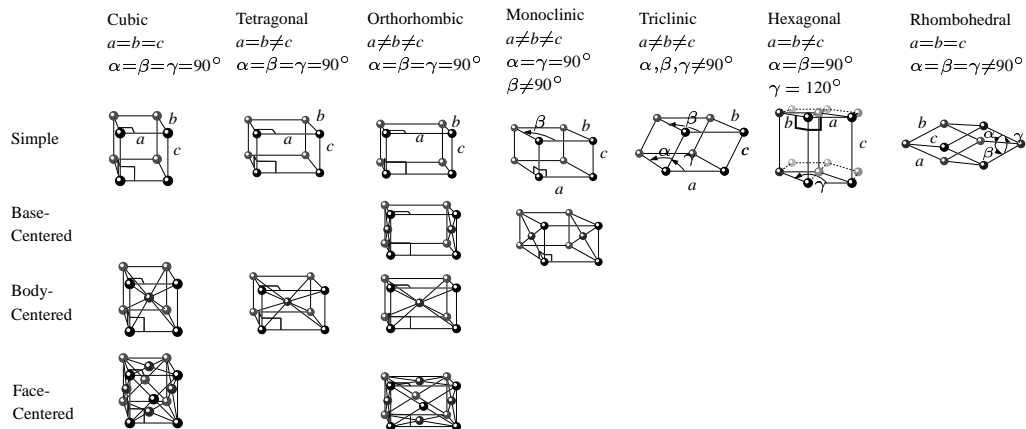


Figure 4.5: The 14 three-dimensional Bravais lattices. The two centered cubic lattices and hexagonal lattice are particularly important in solid state physics. (from Marder's text)

¹For a general crystal structure, there are 32 point groups and 230 space groups that a lattice with a basis can have.

Cubic crystals

There are 3 lattices in the cubic system: the simple cubic (sc) lattice, the body-centered cubic (bcc) lattice, and the face-centered cubic (fcc) lattice. The simplest lattice in three dimensions is the simple cubic lattice. In fact, real crystals of atoms are rarely simple cubic as its packing fraction is only $\pi/6$. The bcc lattice is a simple cubic lattice where there is an additional point in the very center of the cube. A primitive unit cell of the bcc lattice with the cube edge a can be obtained in terms of primitive basis vectors

$$\mathbf{a}_1 = \frac{a}{2}(\hat{\mathbf{x}} + \hat{\mathbf{y}} - \hat{\mathbf{z}}); \quad \mathbf{a}_2 = \frac{a}{2}(-\hat{\mathbf{x}} + \hat{\mathbf{y}} + \hat{\mathbf{z}}); \quad \mathbf{a}_3 = \frac{a}{2}(\hat{\mathbf{x}} - \hat{\mathbf{y}} - \hat{\mathbf{z}}), \quad (4.2)$$

where $\hat{\mathbf{x}}$, $\hat{\mathbf{z}}$, $\hat{\mathbf{x}}$ are the Cartesian unit vectors. The coordination number of a lattice (frequently called Z or z) is the number of nearest neighbors any point of the lattice has. For the bcc lattice the coordination number is $Z = 8$.

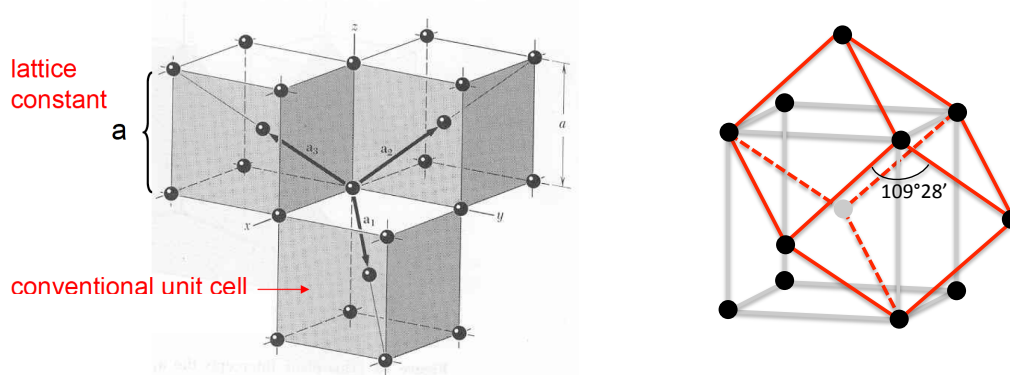


Figure 4.6: Left: primitive basis vectors of the bcc lattice. Right: The bcc lattice with a rhombohedra primitive unit cell of edge $\frac{\sqrt{3}}{2}a$.

The fcc lattice is a simple cubic lattice where there is an additional point in the center of every face of every cube. Analogous to the bcc case, it is sometimes convenient to think of the fcc lattice as a simple cubic lattice with a basis of four atoms per conventional cell. The rhomboheoral primitive cell of the face-centered cubic crystal can be constructed by three primitive translation vectors \mathbf{a}_1 , \mathbf{a}_2 and \mathbf{a}_3 which connect the lattice point at the origin with lattice points at the face centers, i.e,

$$\mathbf{a}_1 = \frac{a}{2}(\hat{\mathbf{x}} + \hat{\mathbf{y}}); \quad \mathbf{a}_2 = \frac{a}{2}(\hat{\mathbf{y}} + \hat{\mathbf{z}}); \quad \mathbf{a}_3 = \frac{a}{2}(\hat{\mathbf{z}} + \hat{\mathbf{x}}). \quad (4.3)$$

The angles between the axes. are 60° . The fcc Bravais lattice has a cubic

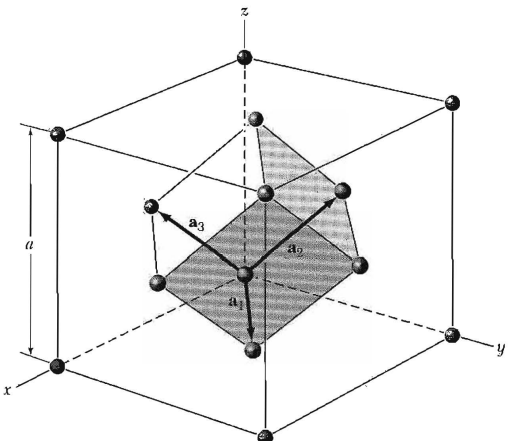


Figure 4.7: The rhombohedral primitive cell of the face-centered cubic crystal.

closest packed structure. The 2D lattice in the plane perpendicular to the [111] direction forms a triangular structure. The lattice points of the second layer is located on half of the holey sites in the first layer. The points of the third layer directly overlay the other half of the first-layer holey sites. The repeating order of the layers is the "ABC...A" stacking as illustrated in Fig. 4.8.

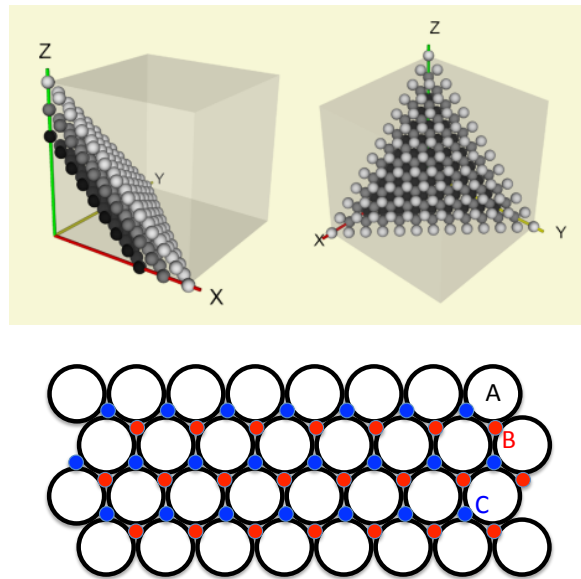


Figure 4.8: "ABC...A" stacking of the fcc lattice. Small red and blue circles denote the locations of layer B and layer C, respectively.

Only slightly more complicated than the simple cubic lattice are the

tetragonal and orthorhombic lattices where the axes remain perpendicular, but the primitive lattice vectors may be of different lengths. The orthorhombic unit cell has three different lengths of its perpendicular lattice primitive basis vectors, whereas the tetragonal unit cell has two lengths the same and one different.

Examples of crystal structure

4.3 The reciprocal lattice in 3D

Definition of reciprocal lattice

The important physics of waves such as vibrational waves, electron waves or electromagnetic waves in solids is best described in reciprocal space as atoms form crystalline order in solids. Consider plane waves $e^{i\mathbf{k}\cdot\mathbf{r}}$ traveling in a Bravais lattice composed of points \mathbf{R} . The set of all vectors \mathbf{G} which yield plane waves $e^{i\mathbf{G}\cdot\mathbf{r}}$ with the periodicity of the Bravais lattice is known as its *reciprocal lattice*. In other words, if

$$e^{i\mathbf{G}\cdot(\mathbf{r}+\mathbf{R})} = e^{i\mathbf{G}\cdot\mathbf{r}}, \quad (4.4)$$

then \mathbf{G} belongs to the reciprocal lattice of the Bravais lattice. Factoring out $e^{i\mathbf{G}\cdot\mathbf{r}}$, we therefore have the definition of the reciprocal lattice of a given direct lattice composed of lattice points \mathbf{R} :

\mathbf{G} is a point in the reciprocal lattice if and only if

$$e^{i\mathbf{G}\cdot\mathbf{R}} = 1. \quad (4.5)$$

Recall that $\mathbf{R} = n_1\mathbf{a}_1 + n_2\mathbf{a}_2 + n_3\mathbf{a}_3$. The primitive basis vectors of the reciprocal lattice \mathbf{b}_i ($i = 1, 2$, and 3) can be chosen through the following conditions:

$$\mathbf{a}_i \cdot \mathbf{b}_j = 2\pi\delta_{ij}, \quad (4.6)$$

where δ_{ij} is the Kronecker delta.² It is obvious that we can generate the primitive basis vectors \mathbf{b}_i as follows:

$$\mathbf{b}_1 = 2\pi \frac{\mathbf{a}_2 \times \mathbf{a}_3}{\mathbf{a}_1 \cdot (\mathbf{a}_2 \times \mathbf{a}_3)}, \quad \mathbf{b}_2 = 2\pi \frac{\mathbf{a}_3 \times \mathbf{a}_1}{\mathbf{a}_1 \cdot (\mathbf{a}_2 \times \mathbf{a}_3)}, \quad \mathbf{b}_3 = 2\pi \frac{\mathbf{a}_1 \times \mathbf{a}_2}{\mathbf{a}_1 \cdot (\mathbf{a}_2 \times \mathbf{a}_3)},$$

where $\mathbf{a}_1 \cdot (\mathbf{a}_2 \times \mathbf{a}_3)$ is the volume of the rhombohedron defined by \mathbf{a}_i . For an arbitrary point in reciprocal space written as

$$\mathbf{G} = m_1\mathbf{b}_1 + m_2\mathbf{b}_2 + m_3\mathbf{b}_3 \quad (4.7)$$

²The Kronecker delta is defined as $\delta_{ij} = 1$ for $i = j$ and $\delta_{ij} = 0$ otherwise.

with m_1 , m_2 , and m_3 integers, \mathbf{G} is a point of the reciprocal lattice because $e^{i\mathbf{G} \cdot \mathbf{R}} = e^{i(m_1 n_1 + m_2 n_2 + m_3 n_3)2\pi} = 1$ is satisfied.

The Reciprocal Lattice as a Fourier Transform

Generally one can think of the reciprocal lattice as being the Fourier transform of a direct lattice. We first prove this statement for the one-dimensional case of which the direct lattice is given by $R_n = na$ and the density $\rho(x)$ of lattice points in one dimension can be expressed as a delta-function of density at these lattice points,

$$\rho(x) = \sum_{n=-\infty}^{\infty} \delta(x - na). \quad (4.8)$$

We can express $\rho(x)$ in terms of the Fourier series as

$$\rho(x) = \sum_{m=-\infty}^{\infty} c_m e^{i\frac{2\pi}{a}mx}, \quad (4.9)$$

and the coefficient c_m is

$$\begin{aligned} c_m &= \frac{1}{a} \int_{-a/2}^{a/2} dx \rho(x) e^{-i\frac{2\pi}{a}mx} \\ &= \frac{1}{a} \int_{-a/2}^{a/2} dx \sum_{n=-\infty}^{\infty} \delta(x - na) e^{-i\frac{2\pi}{a}mx} \\ &= \frac{1}{a}. \end{aligned}$$

Then the Fourier transform of the direct lattice $\rho(x)$ is³

$$\begin{aligned} \mathcal{F}[\rho(x)] &= \int_{x=-\infty}^{\infty} dx e^{ikx} \rho(x) \\ &= \frac{1}{a} \int_{x=-\infty}^{\infty} dx e^{ikx} \sum_{m=-\infty}^{\infty} e^{-i\frac{2\pi}{a}mx} \\ &= \frac{1}{a} \sum_{m=-\infty}^{\infty} \int_{x=-\infty}^{\infty} dx e^{i(k - \frac{2\pi}{a}m)x} \\ &= \frac{2\pi}{a} \sum_{m=-\infty}^{\infty} \delta(k - \frac{2\pi}{a}m). \end{aligned}$$

³Note that $\sum_{m=-\infty}^{\infty} e^{i\frac{2\pi}{a}mx} = \sum_{m=-\infty}^{\infty} e^{-i\frac{2\pi}{a}mx}$ and $\delta(k) = \frac{1}{2\pi} \int_{x=-\infty}^{\infty} dx e^{ikx}$

On the other hand,

$$\begin{aligned}\mathcal{F}[\rho(x)] &= \int_{x=-\infty}^{\infty} dx e^{ikx} \rho(x) \\ &= \sum_{n=-\infty}^{\infty} \int_{x=-\infty}^{\infty} dx e^{ikx} \delta(x - na) \\ &= \sum_{n=-\infty}^{\infty} e^{ikna}.\end{aligned}$$

So

$$\mathcal{F}[\rho(x)] = \sum_{n=-\infty}^{\infty} e^{ikna} = \frac{2\pi}{a} \sum_{m=-\infty}^{\infty} \delta(k - \frac{2\pi}{a}m). \quad (4.10)$$

Thus one obtains that delta function in reciprocal space peaks precisely at the positions of reciprocal lattice vectors. The Fourier transform of the lattice function of the direct lattice is proportional to the lattice function of the reciprocal lattice with the reciprocal constant $G = 2\pi/a$. This proof can be generalized to the 3D case,⁴

$$\mathcal{F}[\rho(\mathbf{r})] = \sum_{\mathbf{R}} e^{i\mathbf{k}\cdot\mathbf{R}} = \frac{(2\pi)^3}{v} \sum_{\mathbf{G}} \delta^3(\mathbf{k} - \mathbf{G}) \quad (4.11)$$

where v is the volume of the unit cell. Note that the reciprocal lattice of an fcc direct lattice is a bcc lattice in reciprocal space. Conversely, the reciprocal lattice of a bcc direct lattice is an fcc lattice in reciprocal space.

Brillouin zone

In order to describe waves in solids, it is important to understand the structure of reciprocal space. A unit cell of the reciprocal lattice is called a Brillouin zone. The Wigner-Seitz primitive cell of the reciprocal lattice is known as the *first Brillouin zone*. Note that term "first Brillouin zone" is only applied to the reciprocal space. In particular when the first Brillouin zone of a particular r -space lattice is referred, what is meant is the Wigner-Seitz primitive cell of the associated reciprocal lattice. For example, the first Brillouin zones of the fcc lattice is just the bcc Wigner-Seitz cell, and the first Brillouin zones of the bcc lattice is just the fcc Wigner-Seitz cell, as shown Fig. 4.9.

⁴Note that $\delta^3(\mathbf{k} - \mathbf{G}) = \delta(k_x - G_x)\delta(k_y - G_y)\delta(k_z - G_z)$

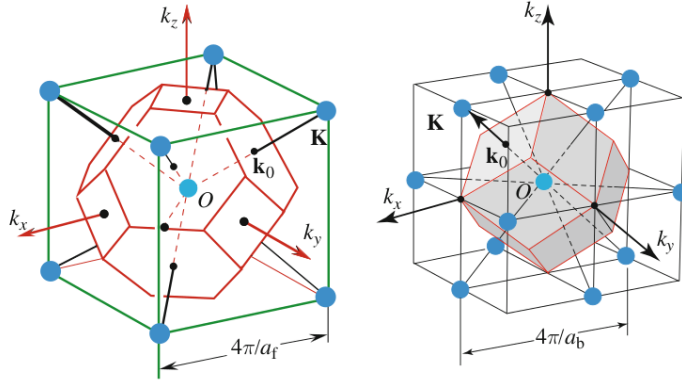


Figure 4.9: First Brillouin zones of the fcc lattice (left) and the bcc (right) lattice.

Lattice planes

Another way to understand the reciprocal lattice is via families of lattice planes of the direct lattice. We first consider a reciprocal lattice vector $\mathbf{G}_{hkl} \equiv h\mathbf{b}_1 + k\mathbf{b}_2 + l\mathbf{b}_3$. In order to satisfy the definition of reciprocal lattice $e^{i\mathbf{G} \cdot \mathbf{R}} = 1$, we have

$$\mathbf{G}_{hkl} \cdot \mathbf{r} = 2\pi m,$$

where m is an integer. Thus a set of collinear reciprocal lattice vectors \mathbf{G}_{hkl} define a family of equally spaced lattice planes to which \mathbf{G}_{hkl} are normal. This family of planes together contain all the points of the 3D Bravais lattice. For \mathbf{r}_1 and \mathbf{r}_2 being separately in two adjacent planes of this family of parallel planes and $\mathbf{G} = G\hat{\mathbf{n}}$ with $\hat{\mathbf{n}}$ being its unit vector, we have

$$G\hat{\mathbf{n}} \cdot (\mathbf{r}_1 - \mathbf{r}_2) = 2\pi\Delta m,$$

where $\hat{\mathbf{n}} \cdot (\mathbf{r}_1 - \mathbf{r}_2) \equiv d_{hkl}$ is the spacing between these two adjacent planes. The shortest reciprocal lattice vector \mathbf{G}_{\min} in the direction $\hat{\mathbf{n}}$ corresponds to $\Delta m = 1$ and gives rise to

$$d_{hkl} = \frac{2\pi}{|\mathbf{G}_{\min}|}, \quad (4.12)$$

with $\mathbf{G}_{\min} = h\mathbf{b}_1 + k\mathbf{b}_2 + l\mathbf{b}_3$ in which h, k , and l do not have a common integer factor other than ± 1 .

The correspondence between reciprocal lattice vectors and families of lattice planes provides a convenient way to specify the orientation of a lattice plane. For a given direction $\hat{\mathbf{n}}$, the indices (h, k, l) which define the shortest reciprocal lattice vector \mathbf{G}_{\min} in the direction are general used to specify the plane orientation. These conventional notations (h, k, l) which have no

common factor are known as Miller Indices. For fcc and bcc lattices, Miller indices are usually stated using the primitive basis vectors of the cubic lattice rather than the primitive basis vector of the fcc or bcc. It is straightforward to show that the interlayer spacing for an orthorhombic lattice is

$$\frac{1}{d_{hkl}} = \sqrt{\frac{h^2}{a_1^2} + \frac{k^2}{a_2^2} + \frac{l^2}{a_3^2}} \quad (4.13)$$

A useful shortcut for figuring out the geometry of lattice planes is to look at the intersection of a plane with the three coordinate axes. The plane intercepts the axes at the points $x_1\mathbf{a}_1$, $x_2\mathbf{a}_2$, and $x_3\mathbf{a}_3$. Since $\mathbf{G} \cdot (x_1\mathbf{a}_1) = 2\pi m$, the Miller indices are inversely proportional to the x_i

$$\frac{1}{x_1} : \frac{1}{x_2} : \frac{1}{x_3} = h : k : l. \quad (4.14)$$

This is the crystallographic definition of the Miller indices as demonstrated in Fig. 4.10.

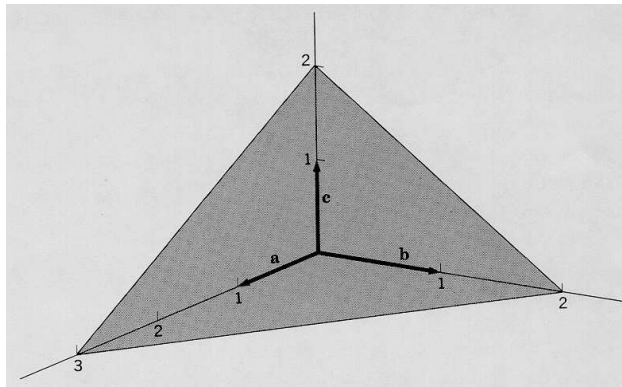


Figure 4.10: An illustration of the crystallographic definition of the Miller indices.

Chapter 5

Wave Scattering by Crystals

Propagation of electron or phonon waves in a crystal plays an important role in underlying physics of materials. Due to the wave-like nature of both the electron and the phonon, they share a similarity in the energy dispersion in reciprocal space. Much of the same physics occurs when crystals scatter waves (or particles) that impinge upon a crystal externally. Furthermore one can experimentally determine crystal structures from real-space microscopy or from diffraction to obtain the lattice structures in reciprocal space. Exposing a solid to a wave such as X-ray, neutron or electron, provides us with a great opportunity to reveal its crystalline structure. In fact it can hardly be overstated how important this type of experiment is to science.

5.1 The Laue and Bragg Conditions

Laue diffraction

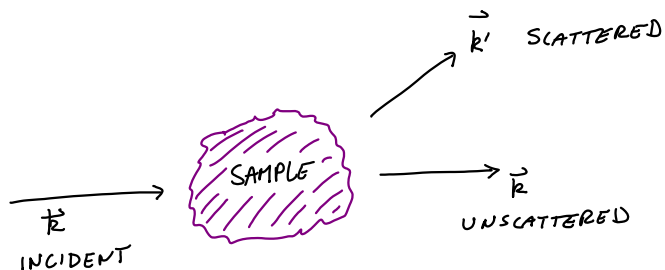


Figure 5.1: A generic scattering experiment (from Simon's text)

For an X-ray being scattered a sample, we can treat the sample as being some potential $V(\mathbf{r})$ that the photon experiences as it goes through the sample, if we think of the incoming X-ray as a particle. According to Fermi's golden rule, the transition rate $\Gamma(\mathbf{k}', \mathbf{k})$ per unit time for the particle scattering from \mathbf{k} to \mathbf{k}' is given by

$$\Gamma(\mathbf{k}', \mathbf{k}) = \frac{2\pi}{\hbar} \left| \langle \mathbf{k}' | V(\mathbf{r}) | \mathbf{k} \rangle \right|^2 \delta(\mathcal{E}_{\mathbf{k}'} - \mathcal{E}_{\mathbf{k}}),$$

where the photon state is $|\mathbf{k}\rangle = \frac{1}{\sqrt{\mathcal{V}}} e^{i\mathbf{k}\cdot\mathbf{r}}$ with \mathcal{V} as being the volume, and the matrix element is nothing but the Fourier transform of the scattering potential because

$$\langle \mathbf{k}' | V(\mathbf{r}) | \mathbf{k} \rangle = \int d\mathbf{r} \frac{e^{-i\mathbf{k}'\cdot\mathbf{r}}}{\sqrt{\mathcal{V}}} V(\mathbf{r}) \frac{e^{i\mathbf{k}\cdot\mathbf{r}}}{\sqrt{\mathcal{V}}} = \frac{1}{\mathcal{V}} \int d\mathbf{r} e^{i\mathbf{Q}\cdot\mathbf{r}} V(\mathbf{r}).$$

Here $\mathbf{Q} \equiv \mathbf{k} - \mathbf{k}'$ is the wave vector change of scattering. If the sample is periodic, the matrix element is zero unless \mathbf{Q} is a reciprocal lattice vector, $\mathbf{Q} = \mathbf{G}$. Assume $V(\mathbf{r})$ periodic such that $V(\mathbf{r} + \mathbf{R}) = V(\mathbf{r})$. The matrix element is

$$\begin{aligned} \langle \mathbf{k}' | V(\mathbf{r}) | \mathbf{k} \rangle &= \frac{1}{\mathcal{V}} \int d\mathbf{r} e^{i\mathbf{Q}\cdot\mathbf{r}} V(\mathbf{r}) \\ &= \frac{1}{\mathcal{V}} \sum_{\mathbf{R}} \int_{\text{unit-cell}} d\mathbf{r} e^{i\mathbf{Q}\cdot(\mathbf{r}+\mathbf{R})} V(\mathbf{r} + \mathbf{R}) \\ &= \frac{1}{\mathcal{V}} \left[\sum_{\mathbf{R}} e^{i\mathbf{Q}\cdot\mathbf{R}} \right] \left[\int_{\text{unit-cell}} d\mathbf{r} e^{i\mathbf{Q}\cdot\mathbf{r}} V(\mathbf{r}) \right] \end{aligned}$$

The first term in the brackets must vanish unless \mathbf{Q} is a reciprocal lattice vector. If $\mathbf{Q} = \mathbf{G}$, the first term in the brackets is the total number of unit cell N and

$$\langle \mathbf{k}' | V(\mathbf{r}) | \mathbf{k} \rangle = \frac{1}{\Omega} \left[\int_{\text{unit-cell}} d\mathbf{r} e^{i\mathbf{Q}\cdot\mathbf{r}} V(\mathbf{r}) \right], \quad (5.1)$$

where Ω is volume of the unit cell in real space, $\Omega = \mathcal{V}/N$. The condition

$$\mathbf{k} - \mathbf{k}' = \mathbf{G}, \quad (5.2)$$

known as the *Laue condition*, is precisely the statement of the conservation of crystal momentum. Also, for elastic scattering, $|\mathbf{k}'| = |\mathbf{k}|$ due to the energy conservation, as enforced by the delta function in the Fermi's golden rule.

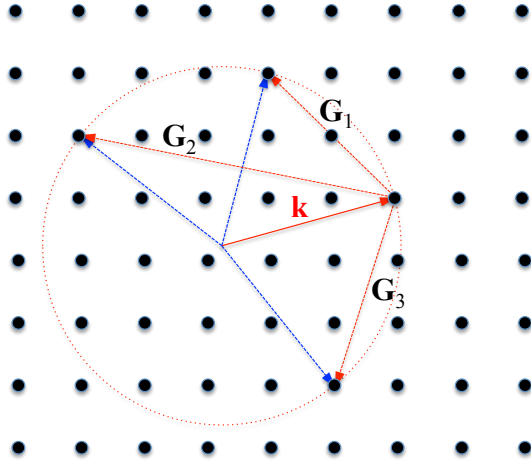


Figure 5.2: Ewald sphere of diffraction

Consider a sphere of radius $|k|$ in momentum space and choose one reciprocal lattice point which lies on the sphere as the origin of the reciprocal space. For any reciprocal lattice points, such as \mathbf{G}_1 , \mathbf{G}_2 and \mathbf{G}_3 , which lie also on the sphere, there will be beams diffracted through constructive interference and emitted along $\mathbf{k} - \mathbf{G}_i$ and the Laue condition is satisfied. This construction of reflection is known as the Ewald construction. This sphere is called *Ewald sphere*.

Bragg reflection

Consider an incoming wave is reflected from two adjacent layers of atoms separated by a distance d as plotted in Fig. 5.3 in which the incidence angle with respect to the atom plane is θ , i.e., the wave is reflected by 2θ . It is obvious that there is a path difference between wave components reflected from the two planes of atoms; the additional distance traveled by the component of the wave that reflects from the further layer of atoms is

$$\text{path difference} = 2d \sin \theta.$$

In order to have constructive interference, this path difference must be equal to an integer number of wavelengths. Thus we derive the Bragg condition

$$2d \sin \theta = n\lambda.$$

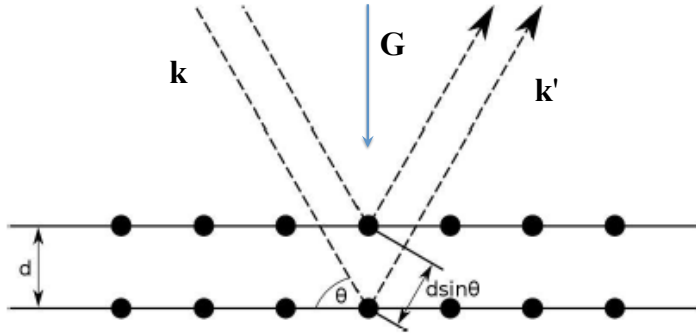


Figure 5.3: Bragg reflection (from Simon's text)

As $\hat{\mathbf{G}}$ is the normal unit vector of the atom planes,

$$\hat{\mathbf{k}} \cdot \hat{\mathbf{G}} = \sin \theta \quad \text{and} \quad \hat{\mathbf{k}}' \cdot \hat{\mathbf{G}} = -\sin \theta.$$

If the Laue condition $\mathbf{k} - \mathbf{k}' = \mathbf{G}$ is satisfied, the relation $\mathbf{k} - \mathbf{k}' = n\mathbf{G}$ also gives rise to a non-vanishing matrix element $\langle \mathbf{k}' | V(\mathbf{r}) | \mathbf{k} \rangle$, where n is an integer. The Laue condition implies that

$$\begin{aligned} |\mathbf{k}|(\hat{\mathbf{k}} - \hat{\mathbf{k}}') &= n\mathbf{G} \\ \frac{2\pi}{\lambda}(\hat{\mathbf{k}} - \hat{\mathbf{k}}') &= n\mathbf{G} \\ \frac{2\pi}{\lambda}(\hat{\mathbf{k}} - \hat{\mathbf{k}}') \cdot \hat{\mathbf{G}} &= n\mathbf{G} \cdot \hat{\mathbf{G}} \\ \frac{2\pi}{\lambda}2\sin \theta &= n\frac{2\pi}{d}. \end{aligned}$$

We use the relation $d = \frac{2\pi}{|\mathbf{G}|}$ in the last step. So we obtain $2d\sin \theta = n\lambda$, showing that the Laue condition is precisely equivalent to the Bragg condition.

Scattering amplitude

The transition rate of wave scattering by a periodic potential is proportional to the matrix element $\langle \mathbf{k}' | V(\mathbf{r}) | \mathbf{k} \rangle$ which can also be expressed as

$$\begin{aligned} \langle \mathbf{k}' | V(\mathbf{r}) | \mathbf{k} \rangle &\propto \frac{1}{V} \left[\sum_{\mathbf{R}} e^{i\mathbf{Q} \cdot \mathbf{R}} \right] S_{(hkl)} \\ S_{(hkl)} &= S(\mathbf{Q}) \equiv \int_{\text{unit-cell}} d\mathbf{r} V(\mathbf{r}) e^{i\mathbf{Q} \cdot \mathbf{r}}, \end{aligned}$$

where $S_{(hkl)}$ is known as the structure factor. Therefore the intensity I_{hkl} of scattering from the lattice planes defined by the reciprocal lattice vector (hkl) is proportional to the square of the structure factor at this reciprocal lattice vector, i.e.,

$$I_{hkl} \propto |S_{(hkl)}|^2.$$

A good approximation assuming the scattering potential is the sum over the scattering potentials of individual atoms,

$$\begin{aligned} V(\mathbf{r}) &= \sum_{\text{atoms } j} V_j(\mathbf{r} - \mathbf{r}_j) \\ &= \sum_{\text{atoms } j} f_j \delta(\mathbf{r} - \mathbf{r}_j) \end{aligned} \quad (5.3)$$

So

$$\begin{aligned} S(\mathbf{Q}) &= \int_{\text{unit-cell}} d\mathbf{r} V(\mathbf{r}) e^{i\mathbf{Q}\cdot\mathbf{r}} \\ &= \sum_{\text{atoms } j} \int_{\text{unit-cell}} d\mathbf{r} f_j \delta(\mathbf{r} - \mathbf{r}_j) e^{i\mathbf{Q}\cdot\mathbf{r}} \\ &= \sum_{\text{atoms } j} f_j e^{i\mathbf{Q}\cdot\mathbf{r}_j}. \end{aligned}$$

For neutron scattering, the *atomic form factor* f_j represents the strength of scattering from nucleus j ; it varies rather erratically with atomic number and is independent of \mathbf{Q} . Also, the structure factor $S(\mathbf{Q})$

In contrast,

Chapter 6

Electrons in a Periodic Potential

The single most important fact that the ions in crystalline solids is that they are in a periodic array. We thus need to consider electrons in a periodic potential $V(\mathbf{r} + \mathbf{R}) = V(\mathbf{r})$. To introduce the basic ideas of band structure, we first discuss the tight-binding approximation.

6.1 Tight-Binding Approximation

We consider a thought experiment in which a very large number of initially isolated atoms are gradually brought together. As a result of their interaction with one another, the energy levels of electrons broaden when the inter-atomic distance is decreased and the electron wavefunctions start to overlap, forming an *energy band*. Under some circumstances, the formation of energy band gives rise to a reduction in electronic energy and consequently leads to chemical bonding. The bandwidth, i.e., the broadening, depends on the overlapping of the wave functions concerned, as illustrated in Fig. 6.1

$$\hat{\mathcal{H}}_A = -\frac{\hbar^2}{2m} \nabla^2 + V_A(\mathbf{r} - \mathbf{R}_n)$$

$$\hat{\mathcal{H}}_A \psi(\mathbf{r} - \mathbf{R}_n) = \varepsilon_{\text{atomic}} \psi(\mathbf{r} - \mathbf{R}_n)$$

For the sake of simplicity, we assume all the atomic orbitals $\psi(\mathbf{r} - \mathbf{R}_n)$ are orthogonal to each other and possess spherical symmetry,

$$\langle \psi(\mathbf{r} - \mathbf{R}_m) | \psi(\mathbf{r} - \mathbf{R}_n) \rangle = \int d\mathbf{r} \psi^*(\mathbf{r} - \mathbf{R}_m) \psi(\mathbf{r} - \mathbf{R}_n) = \delta_{m,n}.$$

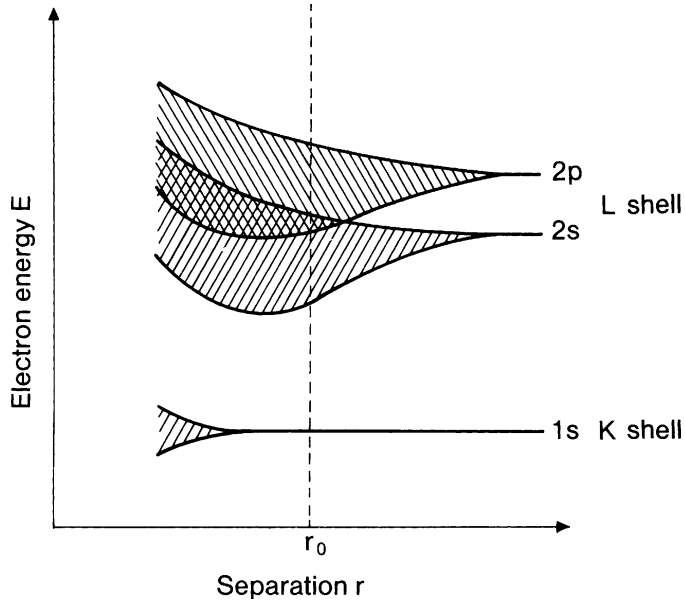


Figure 6.1: Broadening of the energy levels as a large number of identical atoms are gradually brought together. The separation r_0 corresponds to the equilibrium separation of atoms in a solid. (from Ibach & Lüth's text)

The Hamiltonian for an electron in the total potential of all the atoms, i.e., one-electron approximation, can be written as

$$\hat{\mathcal{H}} = -\frac{\hbar^2}{2m} \nabla^2 + V_A(\mathbf{r} - \mathbf{R}_n) + V(\mathbf{r}),$$

where $V(\mathbf{r}) \equiv \sum_{m \neq n} V_A(\mathbf{r} - \mathbf{R}_m)$. We now seek for the eigenfunction $\Psi(\mathbf{r})$ and the eigenenergy \mathcal{E} of the Schrödinger equation

$$\hat{\mathcal{H}}\Psi(\mathbf{r}) = \mathcal{E}\Psi(\mathbf{r})$$

Multiplying the equation by Ψ^* and integrating over the whole crystal, we obtain

$$\mathcal{E} = \frac{\langle \Psi | \hat{\mathcal{H}} | \Psi \rangle}{\langle \Psi | \Psi \rangle},$$

where the Dirac notion is used,

$$\langle \Psi | \hat{\mathcal{H}} | \Psi \rangle = \int d\mathbf{r} \Psi^* \hat{\mathcal{H}} \Psi \quad \text{and} \quad \langle \Psi | \Psi \rangle = \int d\mathbf{r} \Psi^* \Psi$$

Now we exploit the variational method to find ground state by choosing an ansatz solution (trial function) Φ from a linear combination of atomic orbitals $\psi(\mathbf{r} - \mathbf{R}_n)$, i.e.,

$$\Phi(\mathbf{r}) = \sum_n a_n \psi(\mathbf{r} - \mathbf{R}_n).$$

to minimize

$$\frac{\langle \Phi | \hat{\mathcal{H}} | \Phi \rangle}{\langle \Phi | \Phi \rangle}.$$

Provided that there is a translational symmetry in the periodic structure of lattice, one can choose the expansion coefficients as $a_n = e^{i\mathbf{k}\cdot\mathbf{R}_n}$ through introducing with an index \mathbf{k} , and have¹

$$\Psi_{\mathbf{k}} \simeq \Phi_{\mathbf{k}} = \sum_n e^{i\mathbf{k}\cdot\mathbf{R}_n} \psi(\mathbf{r} - \mathbf{R}_n)$$

and

$$\langle \Phi_{\mathbf{k}} | \Phi_{\mathbf{k}} \rangle = \sum_{n,m} e^{i\mathbf{k}\cdot(\mathbf{R}_n - \mathbf{R}_m)} \int d\mathbf{r} \psi^*(\mathbf{r} - \mathbf{R}_m) \psi^*(\mathbf{r} - \mathbf{R}_n).$$

For a sufficiently localized electron, $\psi(\mathbf{r} - \mathbf{R}_n)$ only has significant values around \mathbf{R}_n . To a first-order approximation, we get

$$\langle \Phi_{\mathbf{k}} | \Phi_{\mathbf{k}} \rangle \simeq \sum_n \int d\mathbf{r} \psi^*(\mathbf{r} - \mathbf{R}_n) \psi^*(\mathbf{r} - \mathbf{R}_n) = N,$$

where N is the number of atoms in the crystal. Therefore the eigenenergy is

$$\begin{aligned} \mathcal{E}_{\mathbf{k}} &\simeq \frac{1}{N} \sum_{n,m} e^{i\mathbf{k}\cdot(\mathbf{R}_n - \mathbf{R}_m)} \int d\mathbf{r} \psi^*(\mathbf{r} - \mathbf{R}_m) [\varepsilon_{\text{atomic}} + V(\mathbf{r})] \psi^*(\mathbf{r} - \mathbf{R}_n) \\ &= \varepsilon_{\text{atomic}} + \frac{1}{N} \sum_{n,m} e^{i\mathbf{k}\cdot(\mathbf{R}_n - \mathbf{R}_m)} \int d\mathbf{r} \psi^*(\mathbf{r} - \mathbf{R}_m) V(\mathbf{r}) \psi^*(\mathbf{r} - \mathbf{R}_n) \\ &= \varepsilon_{\text{atomic}} + V_0 + \frac{1}{N} \sum_{n \neq m} e^{i\mathbf{k}\cdot(\mathbf{R}_n - \mathbf{R}_m)} \int d\mathbf{r} \psi^*(\mathbf{r} - \mathbf{R}_m) V(\mathbf{r}) \psi^*(\mathbf{r} - \mathbf{R}_n), \end{aligned}$$

where $V_0 \equiv \int d\mathbf{r} \psi^*(\mathbf{r} - \mathbf{R}_n) V(\mathbf{r}) \psi^*(\mathbf{r} - \mathbf{R}_n)$. If we define the *hopping integral* that depends on \mathbf{k} and describes interaction of electrons at one atomic site with neighbouring sites as

$$t \equiv - \int d\mathbf{r} \psi^*(\mathbf{r} - \mathbf{R}_m) V(\mathbf{r}) \psi^*(\mathbf{r} - \mathbf{R}_n),$$

¹After learning the Bloch's theorem, we will be able to justify the choice of $e^{i\mathbf{k}\cdot\mathbf{R}_n}$ as the expansion coefficients.

one can express the band energy in the tight-binding approximation as

$$\mathcal{E}_{\mathbf{k}} \simeq \varepsilon_{\text{atomic}} + V_0 - t \sum_{\delta} e^{i\mathbf{k}\cdot\delta}, \quad (6.1)$$

where $\delta \equiv \mathbf{R}_n - \mathbf{R}_m$ and the summation \sum_{δ} runs only up to nearest neighbours. This expression shows that the band energy in the tight-binding scheme is mainly given by the energy of original atomic orbitals, plus a constant correction due to interactions, and plus a *hopping term* proportional to the hopping integral t .

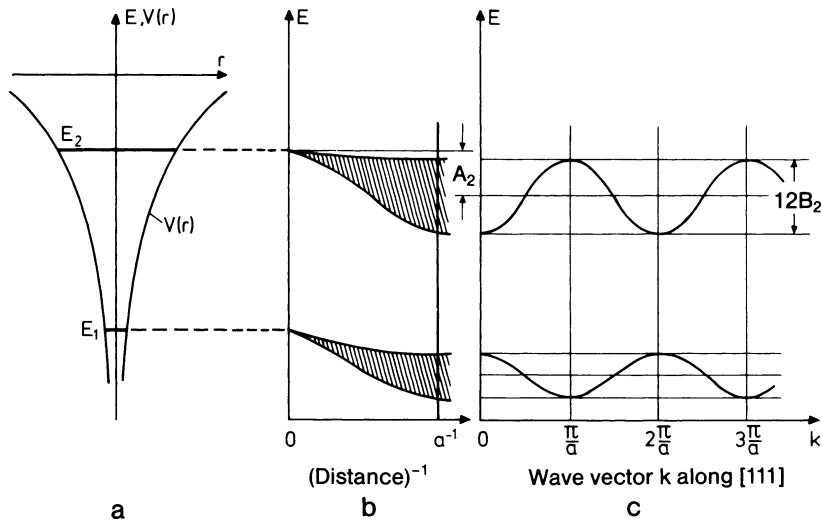


Figure 6.2: Qualitative illustration of the electronic structure in terms of the tight-binding approximation for a primitive cubic lattice of lattice constant a . (from Ibach & Lüth's text)

Zone center ??

Zone boundary $\pm\pi/a$

6.2 The Translational Symmetry – Bloch's theorem

$$\hat{T}_{\mathbf{R}} f(\mathbf{r}) = f(\mathbf{r} + \mathbf{R}). \quad (6.2)$$

$$\begin{aligned}
 \hat{T}_{\mathbf{R}} \hat{\mathcal{H}} \Psi(\mathbf{r}) &= \hat{T}_{\mathbf{R}} \left(-\frac{\hbar^2}{2m} \nabla^2 \Psi(\mathbf{r}) + V(\mathbf{r}) \Psi(\mathbf{r}) \right) \\
 &= -\frac{\hbar^2}{2m} \nabla^2 \Psi(\mathbf{r} + \mathbf{R}) + V(\mathbf{r} + \mathbf{R}) \Psi(\mathbf{r} + \mathbf{R}) \\
 &= -\frac{\hbar^2}{2m} \nabla^2 \Psi(\mathbf{r}) + V(\mathbf{r}) \Psi(\mathbf{r} + \mathbf{R}) \\
 &= \hat{\mathcal{H}} \Psi(\mathbf{r} + \mathbf{R}) \\
 &= \hat{\mathcal{H}} \hat{T}_{\mathbf{R}} \Psi(\mathbf{r})
 \end{aligned} \tag{6.3}$$

$$\hat{T}_{\mathbf{R}} \Psi(\mathbf{r}) = C_{\mathbf{R}} \Psi(\mathbf{r}). \tag{6.4}$$

$$\begin{aligned}
 \hat{T}_{\mathbf{R}+\mathbf{R}'} \Psi(\mathbf{r}) &= \hat{T}_{\mathbf{R}'} \hat{T}_{\mathbf{R}} \Psi(\mathbf{r}) \\
 C_{\mathbf{R}+\mathbf{R}'} \Psi(\mathbf{r}) &= \hat{T}_{\mathbf{R}'} C_{\mathbf{R}} \Psi(\mathbf{r}) \\
 &= C_{\mathbf{R}'} C_{\mathbf{R}} \Psi(\mathbf{r})
 \end{aligned}$$

$$\begin{aligned}
 \langle \Psi(\mathbf{r}) | \Psi(\mathbf{r}) \rangle &= \langle \Psi(\mathbf{r} + \mathbf{R}) | \Psi(\mathbf{r} + \mathbf{R}) \rangle = 1 \\
 &= C_{\mathbf{R}}^* C_{\mathbf{R}} \langle \Psi(\mathbf{r}) | \Psi(\mathbf{r}) \rangle
 \end{aligned} \tag{6.5}$$

$$|C_{\mathbf{R}}|^2 = 1. \tag{6.6}$$

$$C_{\mathbf{R}} = e^{i\mathbf{k}\cdot\mathbf{R}} \tag{6.7}$$

for some real \mathbf{k} . We the have

$$\Psi_{\mathbf{k}}(\mathbf{r} + \mathbf{R}) = e^{i\mathbf{k}\cdot\mathbf{R}} \Psi_{\mathbf{k}}(\mathbf{r}), \tag{6.8}$$

where is \mathbf{k} an index. This is the Bloch’s theorem.

Multiplying Eq ?? by a phase factor $e^{-i\mathbf{k}\cdot\mathbf{r}}$, we get

$$\Psi_{\mathbf{k}}(\mathbf{r} + \mathbf{R}) e^{-i\mathbf{k}\cdot(\mathbf{r} + \mathbf{R})} = e^{-i\mathbf{k}\cdot\mathbf{r}} \Psi_{\mathbf{k}}(\mathbf{r})$$

we can define $e^{-i\mathbf{k}\cdot\mathbf{r}} \Psi_{\mathbf{k}}(\mathbf{r})$ as a function $u_{\mathbf{k}}(\mathbf{r})$ with a periodicity \mathbf{R} , i.e.,

$$u_{\mathbf{k}}(\mathbf{r}) \equiv e^{-i\mathbf{k}\cdot\mathbf{r}} \Psi_{\mathbf{k}}(\mathbf{r})$$

Therefore

$$\begin{aligned} u_{\mathbf{k}}(\mathbf{r} + \mathbf{R}) &= e^{-i\mathbf{k}\cdot(\mathbf{r} + \mathbf{R})} \Psi_{\mathbf{k}}(\mathbf{r} + \mathbf{R}) \\ &= e^{-i\mathbf{k}\cdot(\mathbf{r} + \mathbf{R})} e^{i\mathbf{k}\cdot\mathbf{R}} \Psi_{\mathbf{k}}(\mathbf{r}) \\ &= u_{\mathbf{k}}(\mathbf{r}) \end{aligned} \quad (6.9)$$

$$\Psi_{\mathbf{k}}(\mathbf{r}) = e^{i\mathbf{k}\cdot\mathbf{r}} u_{\mathbf{k}}(\mathbf{r}) \quad (6.10)$$

This is another version of Bloch's theorem; $\Psi_{\mathbf{k}}(\mathbf{r})$ is a *modified "plane"* wave known as the Bloch function. Because $u_{\mathbf{k}}(\mathbf{r})$ is a periodic function, it can be written as a sum over reciprocal lattice vectors,

$$u_{\mathbf{k}}(\mathbf{r}) = \sum_{\mathbf{G}} \tilde{u}_{\mathbf{k}} e^{i\mathbf{G}\cdot\mathbf{r}}. \quad (6.11)$$

Thus the wave function can be expressed as

$$\Psi_{\mathbf{k}}(\mathbf{r}) = \sum_{\mathbf{G}} \tilde{u}_{\mathbf{k}} e^{i(\mathbf{G} + \mathbf{k})\cdot\mathbf{r}}. \quad (6.12)$$

This implies that we can write each eigenstate as being made up of plane-wave states $e^{i\mathbf{k}\cdot\mathbf{r}}$ which differ by reciprocal lattice vectors \mathbf{G} .

Fourier analysis of Bloch's theorem

In any given Bloch wave function, only plane waves with \mathbf{k} that differ by some reciprocal vector \mathbf{G} can be mixed together. To further understand this, we derive the Schrödinger equation in the momentum space. First, consider the Schrödinger equation,

$$\left(-\frac{\hbar^2}{2m} \nabla^2 + V(\mathbf{r}) \right) \Psi(\mathbf{r}) = \mathcal{E} \Psi(\mathbf{r}).$$

We then expand $\Psi(\mathbf{r})$ in terms of plane waves $e^{i\mathbf{k}'\cdot\mathbf{r}}$ and have²

$$\Psi(\mathbf{r}) = \sum_{\mathbf{k}'} \Psi(\mathbf{k}') e^{i\mathbf{k}'\cdot\mathbf{r}}. \quad (6.13)$$

Similarly we express $V(\mathbf{r})$ as

$$V(\mathbf{r}) = \sum_{\mathbf{G}} V_{\mathbf{G}} e^{i\mathbf{G}\cdot\mathbf{r}},$$

² $\Psi(\mathbf{k}')$ is denoted as $\Psi_{\mathbf{k}'}$ in Simion's text.

where \mathbf{G} is the reciprocal lattice vector. The Schrödinger equation becomes

$$\sum_{\mathbf{k}'} \left(\frac{\hbar^2 |\mathbf{k}'|^2}{2m} + V(\mathbf{r}) \right) \Psi(\mathbf{k}') e^{i\mathbf{k}' \cdot \mathbf{r}} = \mathcal{E} \sum_{\mathbf{k}'} \Psi(\mathbf{k}') e^{i\mathbf{k}' \cdot \mathbf{r}}. \quad (6.14)$$

Note that

$$\begin{aligned} \sum_{\mathbf{k}'} V(\mathbf{r}) \Psi(\mathbf{k}') e^{i\mathbf{k}' \cdot \mathbf{r}} &= \sum_{\mathbf{k}' \in \mathbf{G}} V_{\mathbf{G}} e^{i(\mathbf{G} + \mathbf{k}') \cdot \mathbf{r}} \Psi(\mathbf{k}') \\ &= \sum_{\mathbf{k}' \in \mathbf{G}} V_{\mathbf{G}} e^{i(\mathbf{G} + \mathbf{k}' - \mathbf{G}) \cdot \mathbf{r}} \Psi(\mathbf{k}' - \mathbf{G}), \end{aligned}$$

where the summation index \mathbf{k}' is dummy and can be changed from \mathbf{k}' to $\mathbf{k}' - \mathbf{G}$ in the last step. The modified Schrödinger equation is

$$\sum_{\mathbf{k}'} \left\{ \left(\frac{\hbar^2 |\mathbf{k}'|^2}{2m} - \mathcal{E} \right) \Psi(\mathbf{k}') + \sum_{\mathbf{G}} V_{\mathbf{G}} \Psi(\mathbf{k}' - \mathbf{G}) \right\} e^{i\mathbf{k}' \cdot \mathbf{r}} = 0.$$

Since the plane waves $e^{i\mathbf{k}' \cdot \mathbf{r}}$ which satisfy the Born-von Karman boundary condition are orthogonal, the coefficient of each separate term inside $\{ \}$ must vanish. We then have³

$$\left(\mathcal{E} - \frac{\hbar^2 |\mathbf{k}|^2}{2m} \right) \Psi(\mathbf{k}) = \sum_{\mathbf{G}} V_{\mathbf{G}} \Psi(\mathbf{k} - \mathbf{G}). \quad (6.15)$$

This is a representation of the Schrödinger equation in the momentum space. The wave vector \mathbf{k} of the Fourier component $\Psi(\mathbf{k})$ in Eq. 6.13 only assumes the values $\mathbf{k}, \mathbf{k} - \mathbf{K}, \mathbf{k} - \mathbf{K}' \dots$, and $\Psi(\mathbf{k})$ couples only to $\Psi(\mathbf{k} - \mathbf{G})$ whose \mathbf{k} -values differ from one another by a reciprocal vector \mathbf{G} . Therefore the wave function is of the form

$$\Psi_{\mathbf{k}}(\mathbf{r}) = \sum_{\mathbf{G}} \Psi(\mathbf{k} - \mathbf{G}) e^{i(\mathbf{k} - \mathbf{G}) \cdot \mathbf{r}} \quad (6.16)$$

$$\begin{aligned} &= e^{i\mathbf{k} \cdot \mathbf{r}} \sum_{\mathbf{G}} \Psi(\mathbf{k} - \mathbf{G}) e^{-i\mathbf{G} \cdot \mathbf{r}} \\ &\equiv e^{i\mathbf{k} \cdot \mathbf{r}} u_{\mathbf{k}}(\mathbf{r}) \end{aligned} \quad (6.17)$$

³Alternatively one can prove this by multiplying the equation by $\frac{1}{V} e^{-i\mathbf{k} \cdot \mathbf{r}}$ and then integrating over the entire volume V in r -space, i.e.,

$$\sum_{\mathbf{k}'} \frac{1}{V} \int d\mathbf{r} e^{i(\mathbf{k}' - \mathbf{k}) \cdot \mathbf{r}} \left\{ \left(\frac{\hbar^2 |\mathbf{k}'|^2}{2m} - \mathcal{E} \right) \Psi(\mathbf{k}') + \sum_{\mathbf{G}} V_{\mathbf{G}} \Psi(\mathbf{k}' - \mathbf{G}) \right\} = 0.$$

Using the identity $\frac{1}{V} \int d\mathbf{r} e^{i(\mathbf{k}' - \mathbf{k}) \cdot \mathbf{r}} = \delta_{\mathbf{k}, \mathbf{k}'}$, we get Eq. 6.15.

It is obvious that $u_{\mathbf{k}}(\mathbf{r}) = \sum_{\mathbf{G}} \Psi(\mathbf{k} - \mathbf{G}) e^{-i\mathbf{G}\cdot\mathbf{r}}$ is a periodic function with the same period as the that of the potential $V(\mathbf{r})$. So the Bloch's theorem is proven through Fourier analysis.

In the above Fourier analysis, the index \mathbf{k} describes symmetry properties of translation. One can directly label Bloch wave functions with \mathbf{k}_i which span over the entire momentum space. This method of indexing Bloch wave functions is called the *extended zone scheme*. If \mathbf{k} is shifted by a reciprocal vector \mathbf{G} , the Bloch wave function is invariant because

$$\begin{aligned}\Psi_{\mathbf{k}+\mathbf{G}}(\mathbf{r}) &= \sum_{\mathbf{G}'} \Psi(\mathbf{k} + \mathbf{G} - \mathbf{G}') e^{i(\mathbf{k}+\mathbf{G}-\mathbf{G}')\cdot\mathbf{r}} \\ &= \sum_{\mathbf{G}''} \Psi(\mathbf{k} - \mathbf{G}'') e^{i(\mathbf{k}-\mathbf{G}'')\cdot\mathbf{r}} \\ &= \Psi_{\mathbf{k}}(\mathbf{r}),\end{aligned}\tag{6.18}$$

where the summation index $\mathbf{G}'' \equiv \mathbf{G}' - \mathbf{G}$ is dummy. For a given \mathbf{k} , one can find a set of wave functions $\Psi_{\mathbf{k}_1}(\mathbf{r})$, $\Psi_{\mathbf{k}_2}(\mathbf{r})$, $\Psi_{\mathbf{k}_3}(\mathbf{r}) \dots$ with different energies but the same eigenvalue $e^{i\mathbf{k}\cdot\mathbf{R}}$ when acted upon by $\hat{T}_{\mathbf{R}}$. One way to ensure the set of all $\Psi_{\mathbf{k}_i}(\mathbf{r})$ is a complete and linearly independent set of wave functions is by using the *reduced zone scheme*. In the reduced zone scheme, we limit \mathbf{k} to be within the first Brillouin zone. Wave vectors lying outside of the first Brillouin zone will be shifted by a reciprocal vector \mathbf{G} into the aforementioned zone accordingly through $\mathbf{k}_i = \mathbf{k} + \mathbf{G}$. Then we need an additional index n to label Bloch wave functions and associate energies as $\Psi_{n,\mathbf{k}}(\mathbf{r})$ and $\mathcal{E}_{n\mathbf{k}}$.

In summary, the Bloch's theorem leads to a profound consequence that even though the potential that the electron feels from each atom is extremely strong, the electrons still behave almost as if they do not see the atoms at all. They still almost form plane wave eigenstates, with the only modification being the periodic Bloch function $u_{\mathbf{k}}(\mathbf{r})$ and the fact that momentum $\hbar\mathbf{k}$ is now crystal momentum.

Homework:

- (1) Prove $\Psi_{-\mathbf{k}}(\mathbf{r}) = \Psi_{\mathbf{k}}^*(\mathbf{r})$
- (2) Prove $\mathcal{E}_n(-\mathbf{k}) = \mathcal{E}_n(\mathbf{k})$
- (3) Prove $\nabla_{\mathbf{k}} \mathcal{E}_n(\mathbf{k}) = 0$ at $\mathbf{k} = 0$ & $\pm \frac{\mathbf{G}}{2}$, i.e., $\left. \frac{\partial \mathcal{E}_n(\mathbf{k})}{\partial k} \right|_{k=0, \pm \frac{G}{2}} = 0$ in all directions.

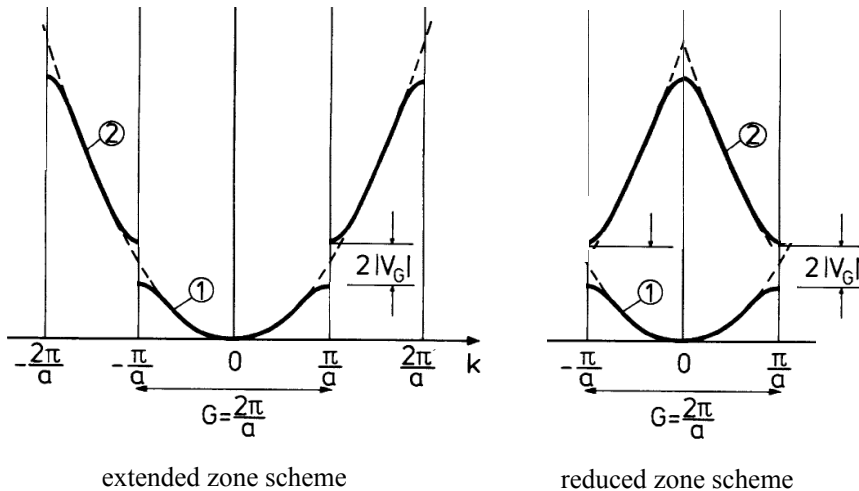


Figure 6.3: Illustration of the extended and reduced zone schemes in one dimension.

6.3 Nearly Free Electrons

After learning the general features of electrons in a Bravais lattice, it is instructive to consider the limiting case of a vanishingly small periodic potential of the ion cores. At the opposite extreme from the tight-binding approximation, the electron states in this approximation are almost the same as free plane waves. This approach is called the nearly-free-electron model, which can often explain the band structure of a crystal and answer almost all the qualitative questions about the behaviour of electrons in metals.

For free electrons in a lattice, the requirement of translational symmetry demands that the possible electronic states are not restricted to a single parabola in \mathbf{k} -space in the reduced zone scheme, but can be equally well described by parabolas shifted by any reciprocal vector \mathbf{G} , i.e.,

$$\Psi_{\mathbf{k}+\mathbf{G}}(\mathbf{r}) = \Psi_{\mathbf{k}}(\mathbf{r}) \quad (6.19)$$

For example, Fig. 6.4 shows the low-lying energy bands of free electron in the empty simple cubic lattice for \mathbf{k} along [100]. Parabolas of the free-electron energy intersect at the zone centre and zone boundaries. The true band structures open up gaps at these \mathbf{k} values. Below we explain this feature by using the nearly-free electron model.

From the Fourier analysis of Bloch's theorem, we know that the Bloch

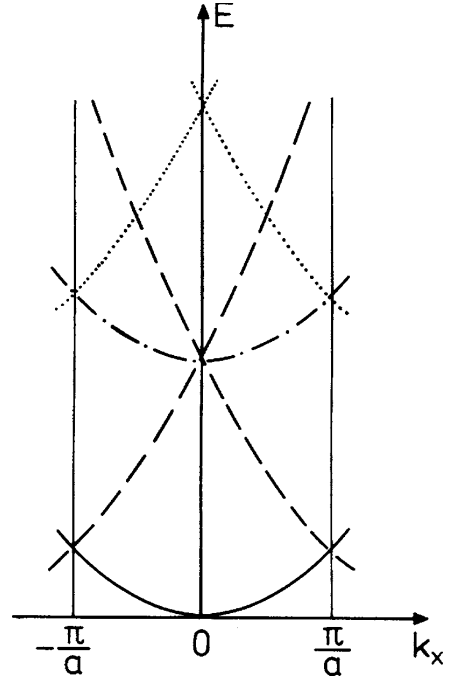


Figure 6.4: The band structure of free electron gas in a sc lattice along k_x in the first Brillouin zone. Various branches stemming from $k^2 = k_x^2 + k_y^2 + k_z^2$ of different $\mathbf{k} = (k_x, k_y, k_z)$ are plotted by various line symbols: (—) for $\mathbf{k} = (k_x, 0, 0)$, (---) for $\mathbf{k} = (k_x \pm \frac{2\pi}{a}, 0, 0)$, (- · -) for $\mathbf{k} = (k_x, \pm \frac{2\pi}{a}, 0)$ and $(k_x, 0, \pm \frac{2\pi}{a})$, (···) for $\mathbf{k} = (k_x \pm \frac{2\pi}{a}, \pm \frac{2\pi}{a}, 0)$, $(k_x \pm \frac{2\pi}{a}, 0, \pm \frac{2\pi}{a})$, and $(k_x, \pm \frac{2\pi}{a}, \pm \frac{2\pi}{a})$

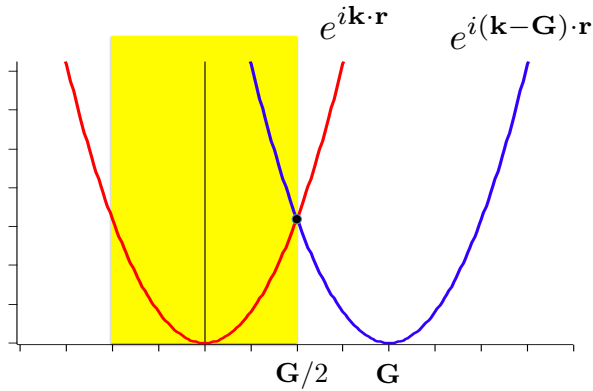


Figure 6.5: Dispersions of $e^{i\mathbf{k}\cdot\mathbf{r}}$ and $e^{i(\mathbf{k}-\mathbf{G})\cdot\mathbf{r}}$ waves

wave function is composed of Fourier components $e^{i(\mathbf{k}-\mathbf{G})\cdot\mathbf{r}}$, i.e.,

$$\Psi_{\mathbf{k}}(\mathbf{r}) = \sum_{\mathbf{G}} \Psi(\mathbf{k} - \mathbf{G}) e^{i(\mathbf{k}-\mathbf{G})\cdot\mathbf{r}}.$$

The nearly-free-electron approximation is equivalent to assuming the wave function is nearly equal to a plane wave, $e^{i\mathbf{k}\cdot\mathbf{r}}$. This means that the leading

term in the expansion is $\Psi(\mathbf{k}) \approx 1$ and higher-order terms of the expansion are negligible.

For a plane wave $e^{i\mathbf{k}\cdot\mathbf{r}}$ travelling near the zone boundary, i.e., $\mathbf{k} \approx \mathbf{G}/2$, the counter-propagating Bragg-reflected wave $e^{i(\mathbf{k}-\mathbf{G})\cdot\mathbf{r}}$ has approximately the same energy and the magnitude as those of $e^{i\mathbf{k}\cdot\mathbf{r}}$. Therefore, in addition to the leading term $\Psi(\mathbf{k}) \approx 1$, we must also keep the terms that include $\Psi(\mathbf{k} - \mathbf{G})$.

In short, because of the presence of the vanishingly small periodic potential, the electron state is no longer a plane wave. Instead, it is a superposition of $e^{i\mathbf{k}\cdot\mathbf{r}}$ and $e^{i(\mathbf{k}-\mathbf{G})\cdot\mathbf{r}}$. We can either use the Schrödinger equations in the k -space or the degenerate perturbation theory to find the eigenstates of nearly-free electrons in a lattice.

using Schrödinger equations in the k -space

Neglecting Fourier components other than $\Psi(\mathbf{k})$ and $\Psi(\mathbf{k} - \mathbf{G})$, the Schrödinger equations in k -space, i.e., Eq. 6.15, become

$$\begin{aligned} \left(\mathcal{E} - \frac{\hbar^2 |\mathbf{k}|^2}{2m} \right) \Psi(\mathbf{k}) &= V_{\mathbf{G}} \Psi(\mathbf{k} - \mathbf{G}) \\ \left(\mathcal{E} - \frac{\hbar^2 |\mathbf{k} - \mathbf{G}|^2}{2m} \right) \Psi(\mathbf{k} - \mathbf{G}) &= V_{-\mathbf{G}} \Psi(\mathbf{k} - \mathbf{G}), \end{aligned} \quad (6.20)$$

where the zero-order correction energy V_0 is constant and can be set to 0. That is, we have

$$\begin{pmatrix} \frac{\hbar^2 |\mathbf{k}|^2}{2m} - \mathcal{E} & V_{\mathbf{G}} \\ V_{-\mathbf{G}} & \frac{\hbar^2 |\mathbf{k} - \mathbf{G}|^2}{2m} - \mathcal{E} \end{pmatrix} \begin{pmatrix} \Psi(\mathbf{k}) \\ \Psi(\mathbf{k} - \mathbf{G}) \end{pmatrix} = 0.$$

We then obtain the secular equation for the energy value

$$\begin{vmatrix} \frac{\hbar^2 |\mathbf{k}|^2}{2m} - \mathcal{E} & V_{\mathbf{G}} \\ V_{-\mathbf{G}} & \frac{\hbar^2 |\mathbf{k} - \mathbf{G}|^2}{2m} - \mathcal{E} \end{vmatrix} = 0.$$

The solutions are

$$\mathcal{E}_{\pm} = \frac{\hbar^2}{4m} (|\mathbf{k}|^2 + |\mathbf{k} - \mathbf{G}|^2) \pm \left[\frac{\hbar^4}{16m^2} (|\mathbf{k} - \mathbf{G}|^2 - |\mathbf{k}|^2)^2 + |V_{\mathbf{G}}|^2 \right]^{1/2}, \quad (6.21)$$

indicating that, near the Brillouin zone boundary, a gap opens up due to scattering by a reciprocal lattice vector.

using degenerate perturbation theory

In this method, we need to solve the eigenvalues and eigenvectors of

$$\hat{\mathcal{H}}|\Psi(\mathbf{r})\rangle = \mathcal{E}|\Psi(\mathbf{r})\rangle,$$

with the Hamiltonian $\hat{\mathcal{H}} = -\frac{\hbar^2}{2m}\nabla^2 + V(\mathbf{r})$. Since the wave function of nearly-free electrons in a lattice is a superposition of $e^{i\mathbf{k}\cdot\mathbf{r}}$ and $e^{i(\mathbf{k}-\mathbf{G})\cdot\mathbf{r}}$, it can be expressed as

$$|\Psi(\mathbf{r})\rangle = \Psi(\mathbf{k})|e^{i\mathbf{k}\cdot\mathbf{r}}\rangle + \Psi(\mathbf{k}-\mathbf{G})|e^{i(\mathbf{k}-\mathbf{G})\cdot\mathbf{r}}\rangle.$$

So the Schrödinger equation is

$$\hat{\mathcal{H}}\left(\Psi(\mathbf{k})|e^{i\mathbf{k}\cdot\mathbf{r}}\rangle + \Psi(\mathbf{k}-\mathbf{G})|e^{i(\mathbf{k}-\mathbf{G})\cdot\mathbf{r}}\rangle\right) = \mathcal{E}\left(\Psi(\mathbf{k})|e^{i\mathbf{k}\cdot\mathbf{r}}\rangle + \Psi(\mathbf{k}-\mathbf{G})|e^{i(\mathbf{k}-\mathbf{G})\cdot\mathbf{r}}\rangle\right).$$

Multiplying both sides of equation with $\langle e^{i\mathbf{k}\cdot\mathbf{r}} |$, we have

$$\Psi(\mathbf{k})\langle e^{i\mathbf{k}\cdot\mathbf{r}} | \hat{\mathcal{H}} | e^{i\mathbf{k}\cdot\mathbf{r}} \rangle + \Psi(\mathbf{k}-\mathbf{G})\langle e^{i\mathbf{k}\cdot\mathbf{r}} | \hat{\mathcal{H}} | e^{i(\mathbf{k}-\mathbf{G})\cdot\mathbf{r}} \rangle = \mathcal{E}\Psi(\mathbf{k})$$

Similarly through the multiplication with $\langle e^{i(\mathbf{k}-\mathbf{G})\cdot\mathbf{r}} |$, we have

$$\Psi(\mathbf{k})\langle e^{i(\mathbf{k}-\mathbf{G})\cdot\mathbf{r}} | \hat{\mathcal{H}} | e^{i\mathbf{k}\cdot\mathbf{r}} \rangle + \Psi(\mathbf{k}-\mathbf{G})\langle e^{i(\mathbf{k}-\mathbf{G})\cdot\mathbf{r}} | \hat{\mathcal{H}} | e^{i(\mathbf{k}-\mathbf{G})\cdot\mathbf{r}} \rangle = \mathcal{E}\Psi(\mathbf{k}-\mathbf{G})$$

We can combine these into a matrix equation,

$$\begin{pmatrix} \langle e^{i\mathbf{k}\cdot\mathbf{r}} | \hat{\mathcal{H}} | e^{i\mathbf{k}\cdot\mathbf{r}} \rangle - \mathcal{E} & \langle e^{i\mathbf{k}\cdot\mathbf{r}} | \hat{\mathcal{H}} | e^{i(\mathbf{k}-\mathbf{G})\cdot\mathbf{r}} \rangle \\ \langle e^{i(\mathbf{k}-\mathbf{G})\cdot\mathbf{r}} | \hat{\mathcal{H}} | e^{i\mathbf{k}\cdot\mathbf{r}} \rangle & \langle e^{i(\mathbf{k}-\mathbf{G})\cdot\mathbf{r}} | \hat{\mathcal{H}} | e^{i(\mathbf{k}-\mathbf{G})\cdot\mathbf{r}} \rangle - \mathcal{E} \end{pmatrix} \begin{pmatrix} \Psi(\mathbf{k}) \\ \Psi(\mathbf{k}-\mathbf{G}) \end{pmatrix} = 0.$$

Because

$$\begin{aligned} \langle e^{i\mathbf{k}\cdot\mathbf{r}} | \hat{\mathcal{H}} | e^{i\mathbf{k}\cdot\mathbf{r}} \rangle &= \frac{\hbar^2|\mathbf{k}|^2}{2m} \\ \langle e^{i(\mathbf{k}-\mathbf{G})\cdot\mathbf{r}} | \hat{\mathcal{H}} | e^{i(\mathbf{k}-\mathbf{G})\cdot\mathbf{r}} \rangle &= \frac{\hbar^2|\mathbf{k}-\mathbf{G}|^2}{2m} \\ \langle e^{i\mathbf{k}\cdot\mathbf{r}} | \hat{\mathcal{H}} | e^{i(\mathbf{k}-\mathbf{G})\cdot\mathbf{r}} \rangle &= V_{-G} \\ \langle e^{i(\mathbf{k}-\mathbf{G})\cdot\mathbf{r}} | \hat{\mathcal{H}} | e^{i\mathbf{k}\cdot\mathbf{r}} \rangle &= V_G, \end{aligned}$$

the matrix equation is

$$\begin{pmatrix} \frac{\hbar^2|\mathbf{k}|^2}{2m} - \mathcal{E} & V_{-G} \\ V_{\mathbf{G}} & \frac{\hbar^2|\mathbf{k}-\mathbf{G}|^2}{2m} - \mathcal{E} \end{pmatrix} \begin{pmatrix} \Psi(\mathbf{k}) \\ \Psi(\mathbf{k}-\mathbf{G}) \end{pmatrix} = 0.$$

Therefore we will obtain the same solutions as those shown by Eq. 6.21.

on the zone boundary

When $\mathbf{k} = \mathbf{G}/2$, free-electron waves of $e^{i\mathbf{k}\cdot\mathbf{r}}$ and $e^{i(\mathbf{k}-\mathbf{G})\cdot\mathbf{r}}$ have exactly the same energy,

$$\frac{\hbar^2|\mathbf{k}|^2}{2m} = \frac{\hbar^2|\mathbf{k} - \mathbf{G}|^2}{2m}$$

and the energy solutions are

$$\mathcal{E}_\pm = \frac{\hbar^2}{2m}|\mathbf{k}|^2 \pm |V_{\mathbf{G}}| \quad (6.22)$$

An energy gap of $|V_{\mathbf{G}}|$ at the zone boundary opens up as a result of Bragg reflection.

Consider a one-dimensional problem of nearly-free electron gas. Let's assume the potential energy is very small and negative near the ion cores, e.g., $V(x) = V \cos(2\pi x/a)$, where $V < 0$ and a is the lattice constant. Note that $V_G < 0$ in this one-dimensional system. Because of translational symmetry, there is a degeneracy of the energy values at the zone edges, $k = \pm \frac{G}{2} = \pm \frac{\pi}{a}$, where two parabolas intersect. To a first-order approximation, the description of the electron states at $k = \pm \frac{\pi}{a}$ is at least a superposition of two corresponding waves,

$$e^{i\frac{\pi}{a}x} \quad \text{and} \quad e^{-i\frac{\pi}{a}x}.$$

If the contributions of wave vectors other than $k = \pm \frac{\pi}{a}$ are neglected, the

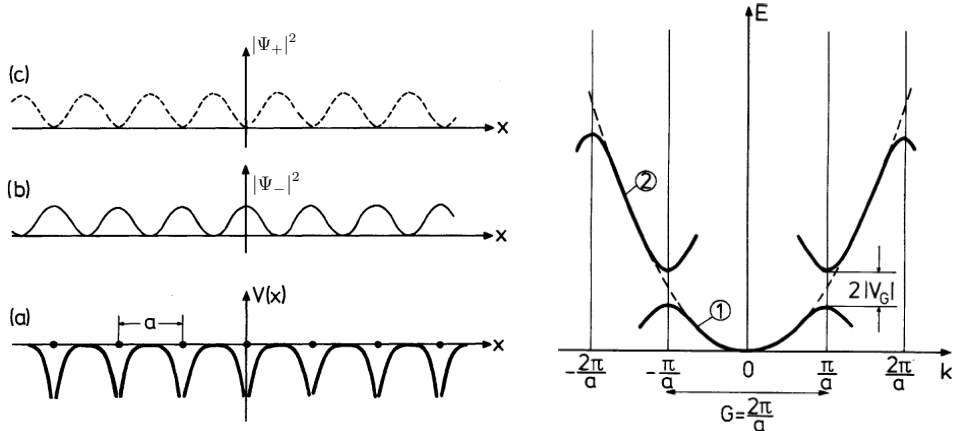


Figure 6.6: Left: (a) The potential energy $V(x)$ of an electron in a one-dimensional lattice. (b) & (c) Probability densities. Right: Splitting of the energy parabola of the free electron at the Brillouin zone edges. (from Ibach & Lüth's text)

energy solutions are

$$\mathcal{E}_\pm = \frac{\hbar^2}{2m} \left(\frac{\pi}{a} \right)^2 \pm |V_G| \equiv \mathcal{E}_0 \pm |V_G|. \quad (6.23)$$

For $\mathcal{E}_+ = \mathcal{E}_0 + |V_G|$, Eq. 6.20 leads us to have

$$|V_G|\Psi\left(\frac{\pi}{a}\right) = V_G\Psi\left(-\frac{\pi}{a}\right)$$

and, because $V_G < 0$, we have the standing wave

$$\Psi_+ \propto (e^{i\frac{\pi}{a}x} - e^{-i\frac{\pi}{a}x}) \propto \sin\left(\frac{\pi}{a}x\right).$$

Similarly we the standing wave

$$\Psi_- \propto (e^{i\frac{\pi}{a}x} + e^{-i\frac{\pi}{a}x}) \propto \cos\left(\frac{\pi}{a}x\right).$$

corresponding to $\mathcal{E}_- = \mathcal{E}_0 - |V_G|$.

If we check the charge densities $|\Psi_\pm|^2$ associated with these two eigenfunctions Ψ_\pm , we see that for an electron in the lower energy eigenstate Ψ_- , the charge density is concentrated mainly around the position of the ion cores and minimum in between; for the higher energy eigenstate Ψ_+ , the charge density is maximum between the cores.

So the general principle is that the periodic potential scatters between the two plane waves $e^{i\mathbf{k}\cdot\mathbf{r}}$ and $e^{i(\mathbf{k}-\mathbf{G})\cdot\mathbf{r}}$. If the energy of these two plane waves are the same, the mixing between them is strong, and the two plane waves can combine to form one state with higher energy (concentrated on the potential maxima) and one state with lower energy (concentrated on the potential minima).

near the zone boundary

For the one-dimensional case, let's assume that $k = \frac{n\pi}{a} + \delta$ and $G = \frac{2\pi n}{a}$ and then we have

$$\begin{aligned} |\mathbf{k}|^2 + |\mathbf{k} - \mathbf{G}|^2 &\approx 2\left(\frac{n\pi}{a}\right)^2 + 2\delta^2 \\ (|\mathbf{k}|^2 - |\mathbf{k} - \mathbf{G}|^2)^2 &\approx 16\left(\frac{n\pi}{a}\delta\right)^2 \end{aligned}$$

and

$$\begin{aligned} \left[\frac{\hbar^4}{16m^2} (|\mathbf{k} - \mathbf{G}|^2 - |\mathbf{k}|^2)^2 + |V_G|^2 \right]^{1/2} &\approx \left[\frac{\hbar^4}{m^2} \left(\frac{n\pi}{a} \delta \right)^2 + |V_G|^2 \right]^{1/2} \\ &\approx |V_G| + \frac{1}{|V_G|} \frac{\hbar^4 \delta^2}{2m^2} \left(\frac{n\pi}{a} \right)^2. \end{aligned}$$

Therefore the energy solutions of Eq. 6.21 are

$$\mathcal{E}_{\pm} \approx \frac{\hbar^2}{2m^2} \left(\frac{n\pi}{a} \right)^2 \pm |V_{\mathbf{G}}| + \frac{\hbar^2\delta^2}{2m} \left[1 \pm \frac{1}{|V_{\mathbf{G}}|} \frac{\hbar^2}{m} \left(\frac{n\pi}{a} \right)^2 \right]$$

6.4 Symmetry in Electronic Band Structure

Chapter 7

Electron-Electron Interactions

7.1 The Hatree-Fock approximation

7.2 Electron-electron interaction: Screening

screened Coulomb potential

7.3 Fermi liquid and quasiparticles

7.4 Electron-phonon interaction

7.5 Electrons in a magnetic Field

Chapter 8

Semiconductor Physics

8.1 Electrons and Holes

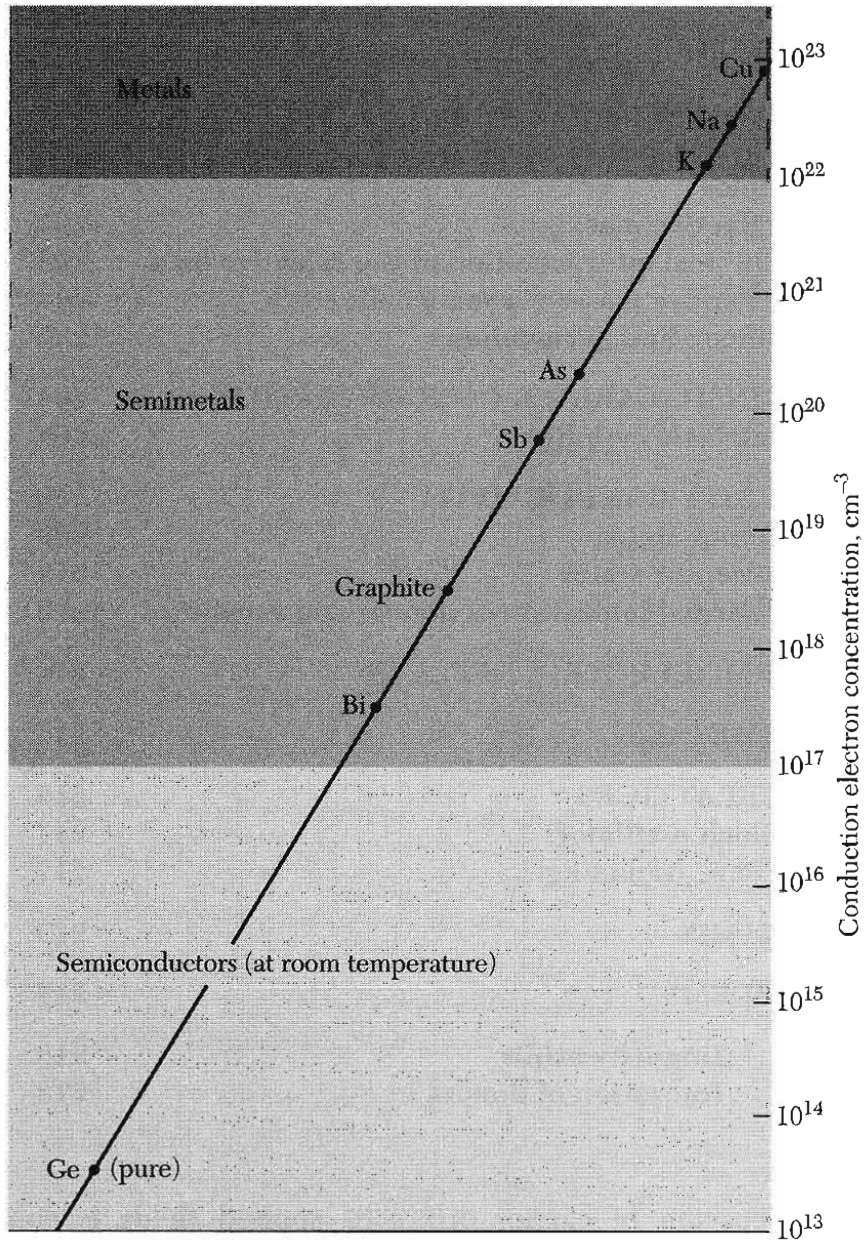


Figure 8.1: Trajectory of a conduction electron scattering off the ion according the naive picture of Drude.

Chapter 9

Magnetism